

Tyrosine and the Oxidative Aggregation of α -Synuclein

Rebecca A. S. Ruf

A dissertation submitted to the faculty of the University of North Carolina at Chapel Hill in partial fulfillment of the requirements for the degree of Doctorate of Philosophy in the Department of Chemistry.

Chapel Hill
2009

Approved by:

Professor Gary J. Pielak, Ph.D.

Professor Matthew R. Redinbo, Ph.D.

Professor Mohanish Deshmukh, Ph.D.

Professor Dorothy Erie, Ph.D.

Professor Garyk Papoian, Ph.D.

©2009
Rebecca A. S. Ruf
ALL RIGHTS RESERVED

Abstract

Rebecca A. S. Ruf: Tyrosine and the Oxidative Aggregation of α -Synuclein
(Under the direction of Professor Gary J. Pielak, Ph.D.)

Oxidative stress and aggregation of the protein α -synuclein are thought to be key factors in Parkinson's disease. Previous work shows that cytochrome *c* plus H_2O_2 causes tyrosine-dependent *in vitro* peroxidative aggregation of proteins, including α -synuclein. Herein, I detail a method for monitoring α -synuclein and cytochrome *c* in a variety of experiments. Using this system, I examine the role of each of α -synuclein's four tyrosine residues and how the protein's conformation affects covalent oxidative aggregation. When α -synuclein adopts a collapsed conformation, tyrosine 39 is essential for wild-type-like covalent aggregation. This lone N-terminal tyrosine, however, is not required for wild type-like covalent aggregation in the presence of a denaturant or when α -synuclein is present in non-covalent fibrils. I also show that pre-formed oxidative aggregates are not incorporated into non-covalent fibrils. These data provide insight as to how dityrosine may be formed in Lewy bodies seen in Parkinson's disease. Additionally, I detail the progress made toward studying the toxicity of α -synuclein aggregates using neuronal microinjection.

To my husband, Ben. You understand my process.

Acknowledgements

Graduate school has simultaneously been one of the most challenging and most rewarding experiences of my life and there are many people to thank for helping me through this journey. To Gary Pielak, your unfailing enthusiasm for this project has kept me going when there was no end in sight. To Mohanish Deshmukh, you planted the seeds of a project that opened my eyes to the world of neurobiology and helped me think about research in a whole new light. Lisa Charlton, you showed me the ropes and have always been the one to keep me looking at the big picture. Without your advice and support I never would have made it this far. To Evan Lutz, the best undergraduate I could have asked for. Teaching you made me a better scientist and your fun-loving attitude made lab entertaining. To Imola Zigoneanu, your meticulous attention to detail averted disaster on several occasions and I'm reassured knowing my project is in your capable hands. Kristin Slade, there's no one else I'd rather have gone on this adventure with. Your dedication to your work continues to be an inspiration to me. And most of all, to my parents, especially my mother, you've always believed I could do anything I set my mind to and pushed me to give nothing less than my best. You are the reason I am who I am today.

Table of Contents

List of Tables.....	ix
List of Figures	x
List of Abbreviations and Symbols	xii
1 Introduction	1
1.1 Causes of Parkinson's disease.....	1
1.1.1 Environmental	1
1.1.2 Genetic.....	3
1.1.3 Age-Related	7
1.2 α -Synuclein.....	8
1.2.1 Lewy Bodies	8
1.2.2 Non-covalent Aggregation	10
1.2.3 Covalent Aggregation	10
1.3 Figures and Tables	13
1.4 References	21
2 Gene Construction and Protein Expression, Purification, and Fluorescent Labeling of Wild-Type and Variant Recombinant Human α -Synuclein and Cytochrome c	37
2.1 Introduction	37
2.2 Materials and Methods	38
2.2.1 Preparation of Mutant Recombinant Human α -Synucleins and Cytochrome c.....	38
2.2.2 Growth, Purification, and Storage of Wild- Type and Variant Recombinant Human α -Synucleins and Cytochromes c	39

2.2.3	Alexa Fluor Labeling of Wild-Type and Variant Recombinant Human α -Synucleins and Cytochrome c	42
2.2.4	Fibril Growth	42
2.3	Results and Discussion	43
2.3.1	Purification of α -Synuclein Labeled with Alexa Fluor Requires a Multi-Step Approach	43
2.3.2	Position of Alexa Fluor 633 on α -Synuclein Does Not Affect α -Synuclein Behavior	44
2.3.3	Alexa Fluor 488 Only Labels Cytochrome c at the Added Cys39, Not at the Endogenous Cys14 or Cys17	45
2.4	Conclusions	46
2.5	Figures and Tables	47
2.6	References	53
3	α -Synuclein Conformation Affects Its Tyrosine-Dependent Oxidative Aggregation	55
3.1	Introduction	55
3.2	Materials and Methods	56
3.2.1	Covalent Aggregation Assays	56
3.2.2	Fibril Formation	56
3.3	Results	57
3.3.1	Alexa Fluor Labeling and Tyrosine-Dependent α -Synuclein Covalent Aggregation	57
3.3.2	Reactivity of the Tyrosines in α -Synuclein to Covalent Aggregation	57

3.2.3	Tyrosine 39 Is Essential for Wild-Type-Like Covalent Aggregation of Native α -Synuclein	58
3.2.4	Changes in Covalent Aggregation Induced by a Denaturant.....	59
3.2.5	Fibril Formation and Oxidative Aggregation	60
3.4	Discussion	60
3.5	Figures and Tables	63
3.6	References	69
4	Progress Towards Neuronal Microinjection of Aggregated α -Synuclein.....	71
4.1	Introduction.....	71
4.2	Sample Preparation	72
4.2.1	Cell Adherence	72
4.2.2	Growth Medium	73
4.2.3	Alexa Fluor Labeling of α -Synuclein	74
4.3	Oxidative Stress Induction and Detection	75
4.3.1	Inducing Oxidative Stress for Positive Control.....	75
4.3.2	Fluorogenic Oxidative Stress Marker Selection.....	76
4.3.3	Staining Procedure	76
4.4	Conclusions	78
4.5	Figures and Tables	79
4.6	References	85

List of Tables

Table 1.1	Chemicals that cause parkinsonism	16
Table 1.2	Genetic causes of Parkinson's disease.	17
Table 2.1	Labeling efficiencies of α -synuclein with Alexa Fluor 633.....	49
Table 4.1	Fluorogenic markers to detect oxidative stress.	81

List of Figures

Figure 1.1	Structures of MPTP, MPP+, and MPPP	13
Figure 1.2	Paraquat redox cycle.....	14
Figure 1.3	Structures of rotenone, dieldrin, and maneb.....	15
Figure 1.4	Incidence rate of Parkinson's disease in Olmsted County, Minnesota from 1976-1990.	18
Figure 1.5	α -Synuclein structure and conformation.	19
Figure 1.6	Representation of amyloid fibril growth.....	20
Figure 2.1	MALDI/MS of α -synuclein with or without Alexa Fluor 633 label.....	47
Figure 2.2	Structure of Alexa Fluor 488 C5 maleimide.	48
Figure 2.3	Position of Alexa Fluor tag does not affect covalent aggregation.	50
Figure 2.4	Alexa Fluor 633 labeled α -synuclein is capable of forming fibrils.	51
Figure 2.5	MALDI/MS of cytochrome c with or without Alexa Fluor 488 label.....	52
Figure 3.1	Alexa Fluor labeling detects peroxidative aggregation.	63
Figure 3.2	Every tyrosine in α -synuclein is reactive, but to varying extents.	64
Figure 3.3	At least one tyrosine on each end is required for wild-type-like covalent aggregation of collapsed α -synuclein	65
Figure 3.4	Tyrosine 39 is not required for full aggregation of denatured α -synuclein.	66
Figure 3.5	Oxidative aggregation interferes with fibril formation.	67
Figure 3.6	α -Synuclein conformation and covalent aggregation.....	68
Figure 4.1	Vitamin E-supplemented growth media modulates neuronal response to oxidative stress.	79
Figure 4.2	Age of stock solution and concentration of working	

	solution affect the ability of TBHP to induce oxidative stress.....	80
Figure 4.3	TBHP causes increased oxidative stress in cells.....	82
Figure 4.4	Transporting cells in staining solution reverses the expected results.	83
Figure 4.5	Transport in hibernation media and staining immediately prior to imaging are crucial for proper oxidative stress detection.	84

List of Abbreviations and Symbols

AD	autosomal dominant
AF488	Alexa Fluor 488
AF633	Alexa Fluor 633
AR	autosomal recessive
C	celsius
cm	centimeters
DAergic	dopaminergic
DTT	dithiolthreitol
<i>E. coli</i>	<i>Escherichia coli</i>
EDTA	ethylenediamine-tetraacetic acid
g	standard gravity
GuHCl	guanidine hydrochloride
h	hours
IAA	iodoacetamide
IPTG	isopropyl- β -D-1-thiogalactopyranoside
kDa	kilodalton
L	liter
LB	Lewy body
LB _{amp}	Luria Broth supplemented with ampicillin
LRRK2	leucine-rich repeat kinase 2
M	molar
MALDI/MS	matrix-assisted laser desorption/ionization mass spectrometry

MEM	minimum essential medium
mg	milligrams
min	minutes
mL	milliliters
mM	millimolar
MPP+	1-methyl-4-phenylpyridinium
MPPP	1-methyl-4-phenyl-4-propionoxy-piperidine
MPTP	1-methyl-4-phenyl-1,2,3,6-tetrahydropyridine
MWCO	molecular weight cutoff
n. a.	not applicable
ng	nanograms
nm	nanometers
NMR	nuclear magnetic resonance spectroscopy
noY	no tyrosine
O.D. ₆₀₀	optical density at 600 nm
PAG	polyacrylamide gel
PBS	phosphate-buffered saline
PC12	pheochromocytoma 12
PD	Parkinson's disease
pink1	PTEN induced putative kinase 1
PMSF	phenylmethanesulphonyl fluoride
ROS	reactive oxygen species
rpm	revolutions per minute

SDS	sodium dodecyl sulfate
SDS-PAGE	sodium dodecyl sulfate polyacrylamide gel electrophoresis
TB _{amp}	terrific broth supplimented with ampicillin
TBHP	tert-butyl-hydroperoxide
Tris	tris(hydroxymethyl) aminomethane
u. k.	unknown
UCH-L1	ubiquitin carboxyl-terminal hydrolase L1
V	volts
v/v	volume/volume
WT	wild-type
α -syn	α -synuclein
μ M	micromolar

Chapter 1 Introduction

Parkinson's disease, the second most common neurodegenerative disorder (1), affects over 1.5 million people in the United States, with over 60,000 new diagnoses each year (2). Parkinson's disease manifests itself in three ways: parkinsonism, death of dopaminergic (DAergic) neurons with a resulting decrease in dopamine levels, and the formation of Lewy bodies (3).

Parkinsonism is a syndrome that encompasses physical symptoms such as bradykinesia (slowed movement), tremor, rigidity, and postural instability. These symptoms arise after the death of 60% - 70% of the DAergic cells in the substantia nigra *pars compacta* (4), which causes an 80% drop in dopamine levels. Lewy bodies are protein inclusions in the remaining neurons. These inclusions have many components, including cytoskeletal proteins such as tubulin (5) and microtubule-associated protein-2 (6), lipids, neurofilaments (7), and cytochrome c (8). The main component of Lewy bodies is α -synuclein (9), much of which is covalently cross-linked. The disease has three main causes: environmental, genetic, and idiopathic (also known as age-related).

1.1 Causes of Parkinson's disease

1.1.1 Environmental

In 1983, the first chemical agent to cause permanent parkinsonism in humans was identified (10). 1-methyl-4-phenyl-1,2,3,6-tetrahydropyridine

(MPTP) is a byproduct of the incorrect synthesis of 1-methyl-4-phenyl-4-propionoxy-piperidine (MPPP), an opioid similar to morphine (Figure 1.1). MPTP readily crosses the blood brain barrier (11), where it is oxidized to 1-methyl-4-phenylpyridinium (MPP⁺, Figure 1.1) by monoamine oxidase B (12). MPP⁺ then enters DAergic cells via the dopamine transporter, where it is trafficked to the mitochondria and inhibits complex I of the electron transport chain (13). This inhibition causes the generation of reactive oxygen species (ROS) such as superoxide (O₂⁻). To date, MPTP is the only chemical agent that reproduces the three hallmarks of Parkinson's disease in animal models (14-16) and causes permanent parkinsonism in humans.

Paraquat, a herbicide, has a structure similar to MPP⁺ (Figure 1.2), and has therefore been investigated as a possible parkinsonian toxin. Paraquat mimics many of the symptoms of Parkinson's in animal models through complex I (17) and complex III (18) inhibition. When complex III is inhibited, it can leak excess electrons to oxygen, resulting in the generation of O₂⁻ (19). Paraquat is an especially potent ROS generator because it undergoes redox cycling using various enzymes in the cell (including complex I and complex III) to generate O₂⁻ and regenerate the paraquat molecule (Figure 1.2). While no confirmed cases of paraquat-induced Parkinson's disease have been reported, epidemiological evidence suggests a higher likelihood of the disease in individuals exposed to paraquat in agricultural settings (20, 21).

Several other pesticides (Figure 1.3) have also been used to replicate Parkinson's in animal models, although none of them reproduce all three of the

hallmarks seen in humans. The insecticide rotenone elucidates symptoms via complex I inhibition (22), but due to its short half life in soil and water (23) and the efficiency which the liver breaks it down (14), it is unlikely to cause parkinsonism in humans. Dieldrin, an insecticide, inhibits complex III (24), causing the generation of O_2^- and cytochrome *c* release (25). No causal relationship has been demonstrated in humans, but postmortem brain samples of Parkinson's disease sufferers show an elevated level of dieldrin compared to cohort samples (26). The fungicide maneb, however, has been shown to cause permanent parkinsonism in humans (27) by complex III inhibition (28).

Regardless of the symptoms they induce in animals or humans, all five of these chemical agents work by inhibition of electron transfer in the mitochondria and the generation of ROS, and their properties are summarized in Table 1.1.

1.1.2 Genetic

While only 5-10% of Parkinson's disease sufferers have a monogenic form of the disease (29), genetic causes have been the most widely studied because they can offer simple insight into the mechanisms of this complicated disease. To date, eleven genes have been identified which, through Mendelian inheritance or spontaneous mutation, either cause Parkinson's disease or increase disease susceptibility (Table 1.2).

α -Synuclein was the first such gene identified, yet its cellular function remains unclear. It appears to regulate dopamine homeostasis by trafficking the dopamine transporter away from the cell surface (30) using the microtubule network (31). α -Synuclein's most striking characteristic, *in vivo* and *in vitro*, is its

propensity to aggregate (32). This aggregation propensity is most affected by protein concentration and conformation. Duplications or triplications of the gene cause earlier onset and increased severity of symptoms in a dose-dependent manner (33-35), and mutations in α -synuclein's promoter region are a risk factor for the idiopathic disease. The three identified point mutations, A30P, A53T, and E46K, all increase the propensity of the affected protein to aggregate *in vitro* (36, 37), and impair the proteasome system *in vivo* (38). Additionally, post-translational modifications of the C-terminus of α -synuclein, such as oxidation or phosphorylation, disrupt the protein's conformation and lead to increased aggregation (39, 40).

Five other Parkinson's disease-associated proteins are involved in protein degradation. Ubiquitin carboxyl-terminal hydrolase L1, UCH-L1, is a ubiquitin hydrolase and E3 ligase which plays a dual role in Parkinson's. The I93M mutation causes autosomal-dominant late-onset Parkinson's (41) by increasing ligase function, which decreases the pool of ubiquitin by causing an accumulation of ubiquitinated α -synuclein (42). Conversely, the S18Y mutation has normal hydrolase function but decreased ligase function (42). This mutation facilitates protein degradation and ubiquitin recycling, which protects against Parkinson's. Parkin is another E3 ligase involved in Parkinson's disease, in which mutations confer a loss of ligase function (43-45) causing autosomal-recessive juvenile and early-onset Parkinson's disease (44). Multiple protein targets of parkin have been identified, including the cytoskeletal proteins α - and β -tubulin (46), which are found in Lewy bodies, and the dopamine transporter (47). Interestingly,

parkin interacts with a glycosylated form of α -synuclein (48) and can ameliorate the cytotoxic effects of α -synuclein overexpression (49, 50). Parkin can also deactivate synphilin-1 (51), which interacts with α -synuclein to promote protein inclusion formation. The inheritable R621C mutation of synphilin-1 does not disrupt its interaction with parkin or α -synuclein, but leads to a decrease in inclusion formation (52). Two other Parkinson's-associated proteins are also involved in lysosomal protein degradation. Atp13A2's normal cellular function is unclear, but in autosomal-recessive juvenile and early-onset Parkinson's disease (53, 54) it is degraded by the proteasome system instead of being inserted into the lysosomal membrane where it normally functions (55). Mutations in β -glucocerebrosidase, a lysosomal glucose metabolism protein, cause the lysosomal storage disorder Gaucher's (56) disease, and confer a susceptibility to Parkinson's disease (57, 58) through an unknown mechanism.

Similar to chemical causes of Parkinson's, mitochondrial function and oxidative stress play a role in genetic causes as well. PTEN induced putative kinase 1, pink1, is a mitochondrial kinase that acts on several protein targets. Mutations in pink1 cause autosomal-recessive early-onset Parkinson's disease (59). Inactivation of pink1 *in vivo* causes oxidative stress-induced apoptosis (60) and pink1 mutations cause respiratory chain malfunctions in patients with Parkinson's (61). Pink1 can phosphorylate parkin, which is then trafficked to the mitochondria, where it induces oxidative stress (62, 63) and causes mitochondrial dysfunction. The mitochondrial serine protease omi is also a phosphorylation target of pink1 (64), and this phosphorylation increases omi's

proteolytic activity (64). Insufficient evidence exists to suggest that the G399S and A141S *omi* mutations are associated with Parkinson's disease in humans (65, 66), but these mutations, and *omi* deletion, cause parkinsonism in mouse models (67, 68). While the link between *dj-1* mutation and autosomal-recessive early-onset Parkinson's disease (69) has been established, its function is less clear. It is most likely involved in oxidative stress protection because it sustains mitochondrial complex I *in vitro* (70) and *dj-1* null mice are more sensitive to MPTP-induced parkinsonism (71).

The least-understood class of Parkinson's disease-associated proteins is those involved in cytoskeletal maintenance. Tau is the major neuronal microtubule-associated protein and binds tubulin to promote assembly of the cytoskeleton (72). In Alzheimer's pathology, hyper-phosphorylation causes tau to aggregate into filaments (73-76), the concentration of which is directly proportional to the severity of dementia (77). Hyper-phosphorylated tau cannot bind tubulin (78) and disrupts microtubules (79, 80). Recently, genomic screening has revealed single nucleotide polymorphisms [all of which are linked to the H1 haplotype (81)] associated with a higher Parkinson's disease risk (82). This association implies some common links between the two neurodegenerative disorders. Mutations in leucine-rich repeat kinase 2, LRRK2, are the most frequent genetic cause of Parkinson's disease, accounting for 3.6% of sporadic cases (83) and 10% of familial cases (84). Its cellular function is unknown, but the protein has numerous domains (85) in addition to a kinase domain, including a WD40 repeat (coordinates multi-protein complexes), a Ras/GTPase domain

(cytoskeleton rearrangement), and a leucine-rich repeat domain. Because it is abundantly expressed throughout the central nervous system (86), LRRK2 most likely performs a basic cellular function, possibly cytoskeletal remodeling using the GTPase domain. Conversely, the kinase domain appears to be most important in Parkinson's because some mutations confer a toxic increase of kinase function *in vitro* (87). Interestingly, for the G2019S mutation, disease penetrance increases from 17% at age 50 to 85% at age 70 (88). This increase suggests that LRRK2 mutations are not a direct cause of Parkinson's, but interact with other age-related cellular processes to confer an increased risk of disease.

1.1.3 Age-Related

Age is the most common risk factor in Parkinson's disease (89). As seen in Figure 1.4, the rate of incidence increases exponentially starting at age 50 (90). Interestingly, advancing age not only increases the risk of developing the disease, but also increases the rate of disease progression. An older age of onset has been correlated to a faster rate of progression for cognitive (91), motor (92, 93), and gait and postural (94) symptoms. These data indicate a synergy between Parkinson's disease and the normal aging process.

While the aging process occurs in every living organism, the mechanisms that lead to aging are not fully understood. Possible sources include mitochondrial mutations (95), chromosomal damage through shortened telomeres (96), inappropriate cross-linking of proteins and other cellular components (97), and a disruption of cellular signaling leading to senescence

(98). Oxidative stress is most likely an underlying cause in all these mechanisms, leading to the “oxidative stress theory” of aging (99), which posits that an increased burden of ROS leads to changes in cellular function and, ultimately, death.

There are many causes of Parkinson’s disease which may act alone or in concert. Whether induced by chemical agents, genetic factors, or general aspects of aging, increased oxidative stress plays a key role in the disease.

1.2 α -Synuclein

α -Synuclein is a 140-amino acid, intrinsically disordered protein (100) with three distinct regions (Figure 1.5A). The N-terminal region is positively charged, the hydrophobic core (also known as the non-amyloid component) comprises residues 61-90, and the C-terminal region is negatively charged. α -Synuclein also has four unevenly distributed tyrosine residues, one (Y39) near the N-terminus and three (Y125, Y133, and Y136) near the C-terminus. Although disordered, the protein adopts a compact state (26-29) wherein the charged termini collapse around the hydrophobic core (Figure 1.5B). Multiple factors are involved in the mechanism of Parkinson’s disease, but both non-covalent and covalent aggregation of α -synuclein are thought to play a key role (101).

1.2.1 Lewy Bodies

Lewy bodies in the substantia nigra are one of the hallmarks of Parkinson’s disease and they form due to the aggregation of α -synuclein. The pathway of Lewy body formation is:

α -synuclein monomer \rightarrow oligomer/protofibril \rightarrow amyloid fibril \rightarrow Lewy body

Some evidence suggests that Lewy bodies are toxic to neurons, either by up-regulating apoptotic factors (102) or impairing the ubiquitin-proteasome system (103), or simply by providing a physical barrier to normal cell trafficking. However, the bulk of the biochemical evidence suggests that it is actually an intermediate species, specifically the annular or ring-shaped form of the protofibril, which is most toxic to neurons. Two of the α -synuclein mutations associated with Parkinson's disease, A30P and A53T, both promote the conversion of monomer to protofibril, and A30P also disfavors the conversion of protofibril to fibril (104). Protofibrils can take on an annular conformation, especially when associated with lipid vesicles (105) or brain-derived membranes (106). Annular protofibrils can permeate membranes, both α -synuclein associated with lipid vesicles (105) and the Alzheimer's protein A β associated with PC12 cells (107). Pre-fibrillar amyloid aggregates of proteins not associated with any known disease are also toxic to cultured cells (108), suggesting that the intermediate protofibril form is a generic cell toxin.

While the main component of Lewy bodies is non-covalently-aggregated α -synuclein, covalent aggregation may also play a role in Lewy body development. Nitrotyrosine, a sign of nitritative stress, has been identified as a component of Lewy bodies (109). The oxidative stress marker dityrosine has also been detected in brain hydrolysates of murine models of Parkinson's disease (110). Understanding the process of Lewy body formation and the

interplay between non-covalent and covalent aggregation in that process is one of the keys to understanding Parkinson's disease.

1.2.2 Non-covalent Aggregation

The α -synuclein fibrils observed in patients with Parkinson's are linear rods, 5-10 nm in diameter, much like those seen in other amyloid diseases (111). The fibrils comprise insoluble cross- β -sheets, and their growth *in vitro* exhibits a sigmoidal time dependence (112) as seen in Figure 1.6. Prior to fibril growth there is a lag, the length of which depends on factors such as protein concentration and pH (113). This lag phase also indicates that the formation of fibrils is a nucleation-dependant process (114, 115). Kinetic analysis of fibril formation reveals that the required nucleus is only a single α -synuclein molecule (111), meaning that the natively disordered monomer must undergo a folding event before being converted into protofibrils. Following the lag is a period of elongation in which fibril concentration increases exponentially and plateaus (111). Fibril growth can be monitored by using thioflavin-T, which experiences a shift in its excitation spectrum when bound to β -sheets in fibrils, allowing it to be selectively excited at 442 nm (116).

1.2.3 Covalent Aggregation

Oxidative stress and α -synuclein play some role in Parkinson's disease. Fenton-chemistry based oxidation systems (i.e., a transition metal plus H_2O_2) have been used extensively *in vitro* in attempts to reproduce *in vivo* covalent aggregation of α -synuclein. This mechanism was initially supported by the observation that metals accelerate the fibrillization of α -synuclein (117), but these

systems are not accurate mimics (118, 119). For instance, although dityrosine (tyrosines with a covalent bond between the 3/5 carbon atoms) is observed in the MPTP Parkinson's disease model, the covalent aggregation induced by several Fenton chemistry systems is tyrosine-independent (119). In fact, the HO• generated by Cu²⁺ plus H₂O₂ impedes dityrosine formation in the Alzheimer's disease protein, Aβ (118).

The cytochrome *c*/H₂O₂ oxidation system (120), referred to here as the peroxidative system, is another model based on possible cellular mechanisms. In times of oxidative stress, ROS are produced in the mitochondria. Cytochrome *c* and ROS can leak into the cytosol (121), possibly aided by pores in the mitochondrial membrane formed by α-synuclein (122). This system is a better model for α-synuclein covalent aggregation for two reasons. First, the peroxidative system causes tyrosine-dependent covalent aggregation of α-synuclein (123), similar to the dityrosine seen in murine models of Parkinson's disease. Second, the peroxidative system causes the direct transfer of a free radical from cytochrome *c* to the acceptor protein (124, 125) without a HO• intermediate.

Studies of environmental, genetic, and age-related causes of Parkinson's disease reveal that both the process of oxidative stress and the aggregation of α-synuclein play key roles in the pathogenesis of the disease. As demonstrated above, much research has been done on each of these processes separately, but little is known about their interaction in Parkinson's disease. My research has

sought to address this disparity by answering two questions. What is the role of each of α -synuclein's tyrosines in the process of oxidative aggregation, and at what stage in the non-covalent aggregation process are covalent aggregates formed?

1.3 Figures and Tables

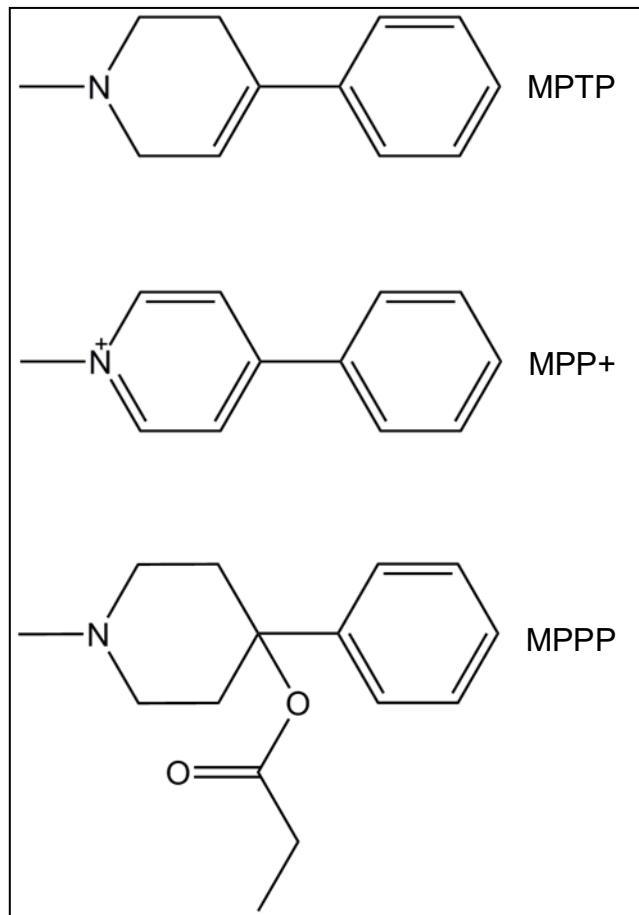


Figure 1.1 Structures of MPTP, MPP+, and MPPP

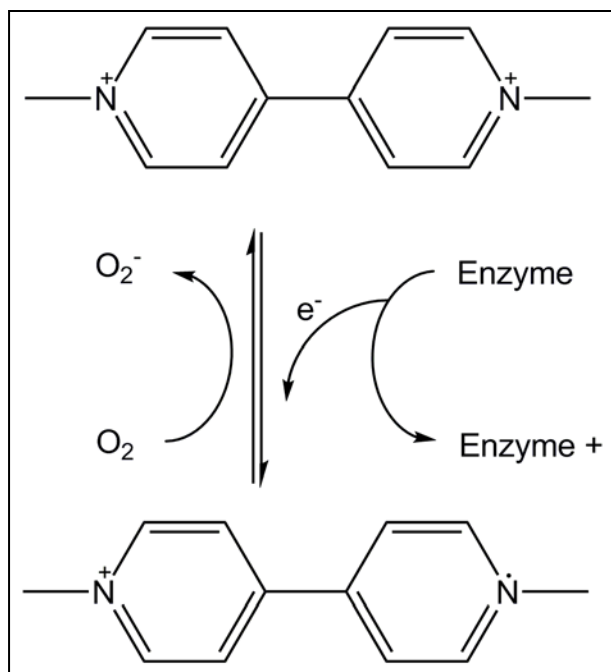


Figure 1.2 Paraquat redox cycle.

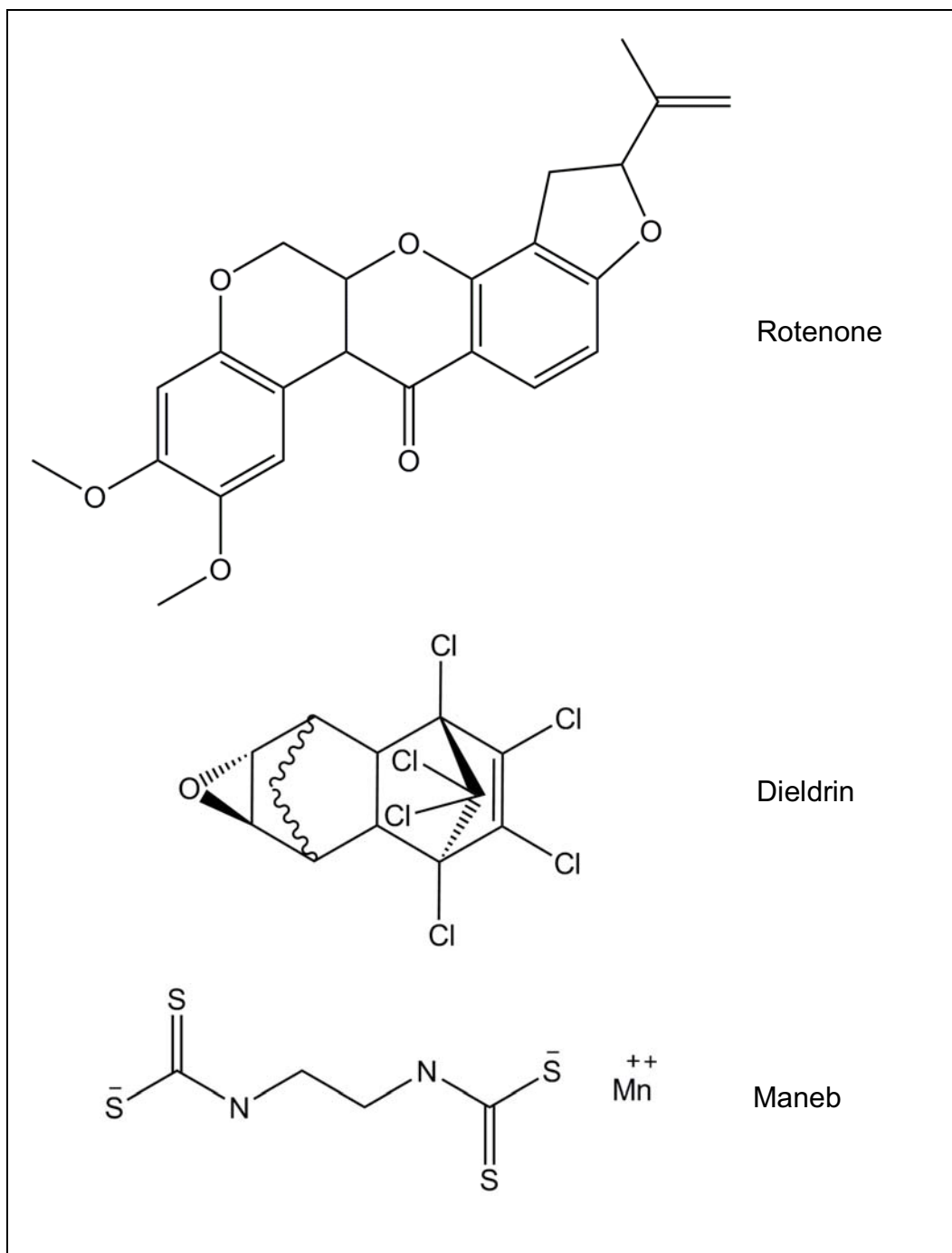


Figure 1.3 Structures of rotenone, dieldrin, and maneb

Chemical	parkinsonism/ Motor defects	DAergic cell death/ [DA] decrease	α -syn aggregation/ LB-like protein aggregates	Mechanism of action	Known damage to humans
MPTP	All parkinsonism symptoms (14)	<i>In vivo</i> cell death and [DA] decrease (15)	None observed (15), except in older monkeys (16)	Mitochondrial complex I inhibition (11)	Permanent parkinsonism (10)
Paraquat	Locomotor deficits (126)	<i>In vitro</i> cell death (65-67)	α -syn positive LB-like aggregates (127)	Mitochondrial complex I (17) and complex III (18) inhibition, O_2^- (19)	Epidemiological evidence (20, 21)
Rotenone	Bradykinesia and rigidity (128)	<i>In vivo</i> cell death (129, 130)	α -syn positive LB-like aggregates (73, 75)	Mitochondrial complex I inhibition (22)	Low probability (14)
Dieldrin	Not studied	<i>In vitro</i> cell death (131)	α -syn fibrillization and aggregation (132, 133)	Mitochondrial complex III inhibition (24), O_2^- and cytochrome <i>c</i> release (25)	Increased levels in PD patients (26)
Maneb	Locomotor deficits (134)	<i>In vivo</i> cell death (134)	Not studied	Mitochondrial complex III inhibition (28)	Permanent parkinsonism (27)

Table 1.1 Chemicals that cause parkinsonism

locus	gene	protein	function	inheritance	onset
PARK1/ PARK4	SNCA	α -synuclein	synaptic dopamine vesicle homeostasis	AD	early
PARK5	UCH-L1	ubiquitin carboxyl-terminal hydrolase L1	ubiquitin hydrolase/ E3 ligase	AD	late
PARK2	Parkin	parkin	ubiquitin E3 ligase	AR	juvenile and early
n. a.	SNCAIP	synphillin-1	interacts with α -synuclein	AD	late
PARK9	ATP13A2	atp13A2	lysosomal function	AR	juvenile and early
n. a.	GBA	β - glucocerebrosidase	lysosomal glucose metabolism	u. k.	u. k.
PARK6	PINK1	PTEN induced putative kinase 1	mitochondrial kinase	AR	early
PARK13	Omi/HtrA2	omi or htrA2	mitochondrial serine protease	AD	u.k.
PARK7	DJ-1	dj-1	oxidative stress protection	AR	early
n. a.	TAU	tau	microtubule assembly	u. k.	u. k.
PARK8	LRRK2	leucine-rich repeat kinase 2/ dardarin	kinase/ cytoskeletal regulation	AD	late

Table 1.2 Genetic causes of Parkinson's disease.

AD = autosomal-dominant, AR = autosomal-recessive, n. a. = not applicable,

u. k. = unknown

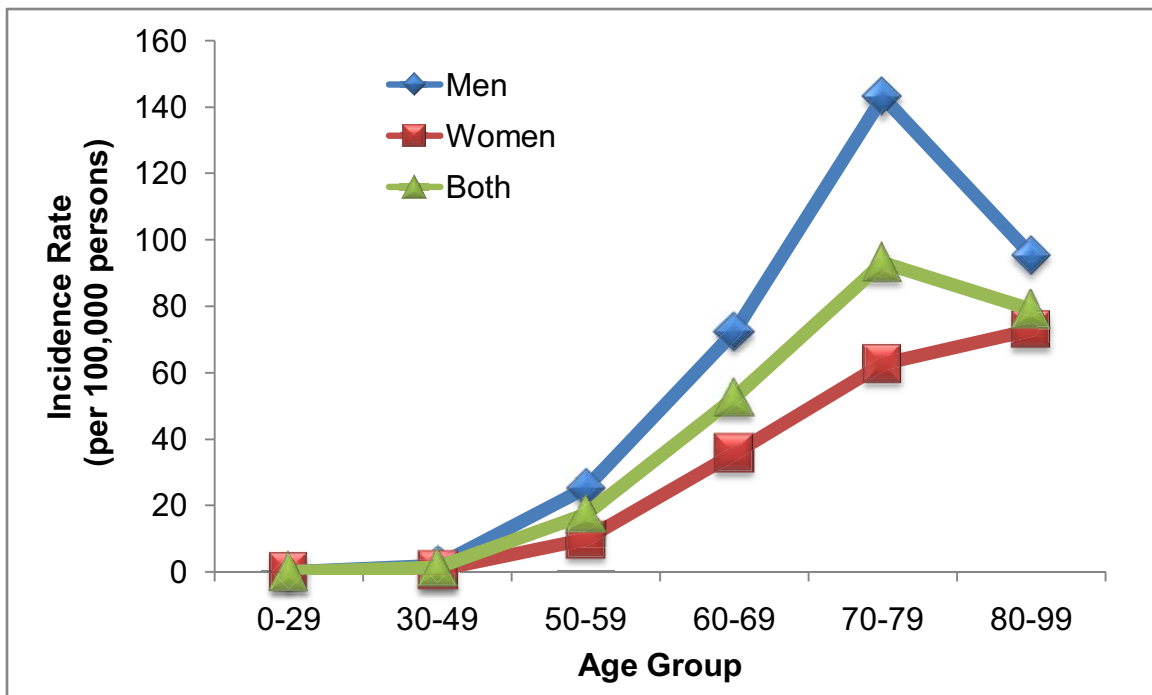


Figure 1.4 Incidence rate of Parkinson's disease in Olmsted County, Minnesota from 1976-1990. Data taken from (90).

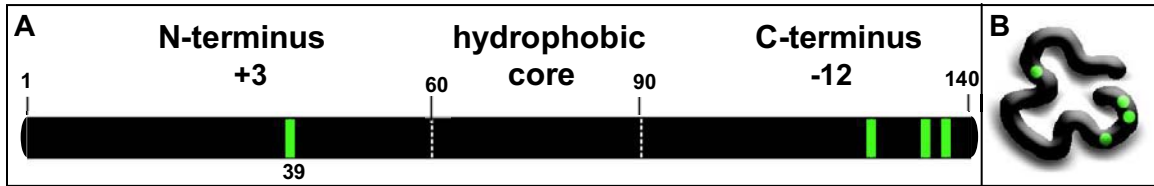


Figure 1.5 α -Synuclein structure and conformation. A schematic representation of α -synuclein's primary structure showing relevant regions, net charges, and position numbers (A), and a cartoon of its collapsed conformation (B). The positions of the tyrosine residues are indicated in green.

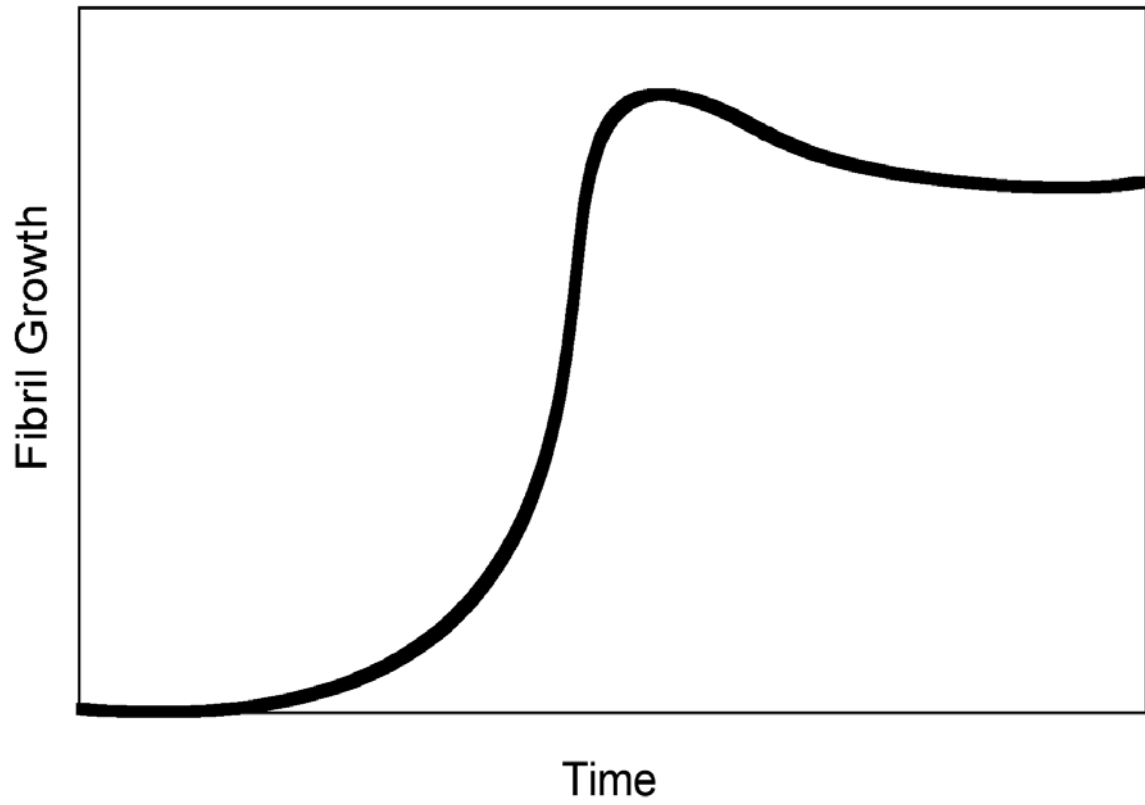


Figure 1.6 Representation of amyloid fibril growth.

1.4 References

1. Hague, S. M., Klaffke, S. and Bandmann, O. (2005) Neurodegenerative disorders: Parkinson's disease and Huntington's disease, *J. Neurol. Neurosurg. Psychiatr.* **76**, 1058-1063.
2. National Parkinson's Foundation
3. Cookson, M. R. (2005) The biochemistry of Parkinson's disease, *Annu. Rev. Biochem.* **74**, 29-52.
4. Lang, A. E. and Lozano, A. M. (1998) Parkinson's disease - first of two parts, *N. Engl. J. Med.* **339**, 1044-1053.
5. Gai, W. P., Power, J. H. T., Blumbergs, P. C., Culvenor, J. G. and Jensen, P. H. (1999) Alpha-synuclein immunoisolation of glial inclusions from multiple system atrophy brain tissue reveals multiprotein components, *J. Neurochem.* **72**, 2093-2100.
6. D'Andrea, M. R., Ilyin, S. and Plata-Salaman, C. R. (2001) Abnormal patterns of microtubule-associated protein-2 (MAP-2) immunolabeling in neuronal nuclei and Lewy bodies in Parkinson's disease substantia nigra brain tissues, *Neurosci. Lett.* **306**, 137-142.
7. Goldman, J. E., Yen, S. H., Chiu, F. C. and Peress, N. S. (1983) Lewy bodies of Parkinson's disease contain neurofilament antigens, *Science* **221**, 1082-1084.
8. Hashimoto, M., Takeda, A., Hsu, L. J., Takenouchi, T. and Masliah, E. (1999) Role of cytochrome *c* as a stimulator of alpha-synuclein aggregation in Lewy body disease, *J. Biol. Chem.* **274**, 28849-28852.
9. Spillantini, M. G., Schmidt, M. L., Lee, V. M. Y., Trojanowski, J. Q., Jakes, R. and Goedert, M. (1997) Alpha-synuclein in Lewy bodies, *Nature* **388**, 839-840.
10. Langston, J. W., Ballard, P., Tetrud, J. W. and Irwin, I. (1983) Chronic parkinsonism in humans due to a product of meperidine-analog synthesis, *Science* **219**, 979-980.

11. Drechsel, D. A. and Patel, M. (2008) Role of reactive oxygen species in the neurotoxicity of environmental agents implicated in Parkinson's disease, *Free Radic. Biol. Med.* **44**, 1873-1886.
12. Heikkila, R. E., Hess, A. and Duvoisin, R. C. (1984) Dopaminergic neurotoxicity of 1-methyl-4-phenyl-1,2,5,6-tetrahydropyridine in mice, *Science* **224**, 1451-1453.
13. Javitch, J. A., D'Amato, R. J., Strittmatter, S. M. and Snyder, S. H. (1985) Parkinsonism-inducing neurotoxin, N-methyl-4-phenyl-1,2,3,6 - tetrahydropyridine: Uptake of the metabolite N-methyl-4-phenylpyridine by dopamine neurons explains selective toxicity, *Proc. Natl. Acad. Sci. U. S. A.* **82**, 2173-2177.
14. Bové, J., Prou, D., Perier, C. and Przedborski, S. (2005) Toxin-induced models of Parkinson's disease, *NeuroRX* **2**, 484-494.
15. Forno, L. S., Delanney, L. E., Irwin, I. and Langston, J. W. (1993) Similarities and differences between MPTP-induced parkinsonism and Parkinson's disease : Neuropathologic considerations, *Adv. Neurol.* **60**, 600-608.
16. Forno, L. S., Langston, J. W., Delanney, L. E., Irwin, I. and Ricaurte, G. A. (1986) Locus ceruleus lesions and eosinophilic inclusions in MPTP-treated monkeys, *Ann. Neurol.* **20**, 449-455.
17. Fukushima, T. T., Yamada, K., Isobe, A., Shiwaku, K. and Yamane, Y. (1993) Mechanism of cytotoxicity of paraquat. I. NADH oxidation and paraquat radical formation via complex I, *Exp. Toxicol. Pathol.* **45**, 354-349.
18. Castello, P. R., Drechsel, D. A. and Patel, M. (2007) Mitochondria are a major source of paraquat-induced reactive oxygen species production in the brain, *J. Biol. Chem.* **282**, 14186-14193.
19. Bus, J. S. and Gibson, J. E. (1984) Paraquat: Model for oxidant-initiated toxicity, *Env. Health Perspect.* **55**, 37-46.

20. Hertzman, C., Wiens, M., Bowering, D., Snow, B. and Calne, D. (1990) Parkinson's disease: A case-control study of occupational and environmental risk factors, *Am. J. Ind. Med.* **17**, 349-355.
21. Liou, H. H., Tsai, M. C., Chen, C. J., Jeng, J. S., Chang, Y. C. and Chen, S. Y. (1997) Environmental risk factors and Parkinson's disease: A case-control study in Taiwan, *Neurology* **48**, 1583-1588.
22. Sherer, T. B., Betarbet, R., Testa, C. M., Seo, B. B., Richardson, J. R., Kim, J. H., Miller, G. W., Yagi, T., Matsuno-Yagi, A. and Greenamyre, J. T. (2003) Mechanism of toxicity in rotenone models of Parkinson's disease, *J. Neurosci.* **23**, 10756-10764.
23. Hisata, J. (2002) Final supplemental environmental impact - lake and stream rehabilitation: Rotenone use and health risks, (Wildlife, W. D. O. F. A.)
24. Bergen, W. G. (1971) The in vitro effect of dieldrin on respiration of rat liver mitochondria, *Proc. Soc. Exp. Biol. Med.* **136**, 732-735.
25. Kitazawa, M., Anantharam, V. and Kanthasamy, A. G. (2001) Dieldrin-induced oxidative stress and neurochemical changes contribute to apoptotic cell death in dopaminergic cells, *Free Radic. Biol. Med.* **31**, 1473-1485.
26. Fleming, L., Mann, J. B., Bean, J., Briggie, T. and Sanchez-Ramos, J. R. (1994) Parkinson's disease and brain levels of organochlorine pesticides, *Ann. Neurol.* **36**, 100-103.
27. Meco, G., Bonifati, V., Vanacore, N. and Fabrizio, E. (1994) Parkinsonism after chronic exposure to the fungicide maneb (manganese ethylene-bis-dithiocarbamate). *Scand. J. Work Environ. Health* **20**, 301-305.
28. Zhang, J., Fitsanakis, V. A., Gu, G., Jing, D., Ao, M., Amarnath, V. and Montine, T. J. (2003) Manganese ethylene-bis-dithiocarbamate and selective dopaminergic neurodegeneration in rat: A link through mitochondrial dysfunction, *J. Neurochem.* **84**, 336-346.
29. Lesage, S. and Brice, A. (2009) Parkinson's disease: From monogenic forms to genetic susceptibility factors, *Hum. Mol. Genet.* **18**, R48-59.

30. Sidhu, A., Wersinger, C. and Vernier, P. (2004) α -Synuclein regulation of the dopaminergic transporter: A possible role in the pathogenesis of Parkinson's disease, *FEBS Lett.* **565**, 1-5.
31. Wersinger, C. and Sidhu, A. (2005) Disruptions of the interaction of α -synuclein with microtubules enhances cell surface recruitment of the dopamine transporter, *Biochemistry* **44**, 13612-13624.
32. Uversky, V. N., Li, J., Souillac, P., Millett, I. S., Doniach, S., Jakes, R., Goedert, M. and Fink, A. L. (2002) Biophysical properties of the synucleins and their propensities to fibrillate, *J. Biol. Chem.* **277**, 11970-11978.
33. Ikeuchi, T., Kakita, A., Shiga, A., Kasuga, K., Kaneko, H., Tan, C.-F., Idezuka, J., Wakabayashi, K., Onodera, O., Iwatsubo, T., Nishizawa, M., Takahashi, H. and Ishikawa, A. (2008) Patients homozygous and heterozygous for SNCA duplication in a family with parkinsonism and dementia, *Arch. Neurol.* **65**, 514-519.
34. Ross, O. A., Braithwaite, A. T., Skipper, L. M., Kachergus, J., Hulihan, M. M., Middleton, L. T., Nishioka, K., Fuchs, J., Gasser, T., Maraganore, D. M., Adler, C. H., Larvor, L., Chartier-Harlin, M.-C., Nilsson, C., Langston, J. W., Gwinn, K., Hattori, N. and Farrer, M. J. (2008) Genomic investigation of alpha-synuclein multiplication and parkinsonism, *Ann. Neurol.* **63**, 743-750.
35. Ibanez, P., Lesage, S., Janin, S., Lohmann, E., Durif, F., Destee, A., Bonnet, A.-M., Brefel-Courbon, C., Heath, S., Zelenika, D., Agid, Y., Durr, A. and Brice, A. (2009) α -Synuclein gene rearrangements in dominantly inherited parkinsonism: Frequency, phenotype, and mechanisms, *Arch. Neurol.* **66**, 102-108.
36. Fredenburg, R. A., Rospigliosi, C., Meray, R. K., Kessler, J. C., Lashuel, H. A., Eliezer, D. and Lansbury, P. T. (2007) The impact of the E46K mutation on the properties of α -synuclein in its monomeric and oligomeric states, *Biochemistry* **46**, 7107-7118.
37. Conway, K. A., Harper, J. D. and Lansbury, P. T. (1998) Accelerated in vitro fibril formation by a mutant alpha-synuclein linked to early-onset Parkinson disease, *Nat. Med.* **4**, 1318-1320.

38. Tanaka, Y., Engelender, S., Igarashi, S., Rao, R. K., Wanner, T., Tanzi, R. E., Sawa, A., L. Dawson, V., Dawson, T. M. and Ross, C. A. (2001) Inducible expression of mutant α -synuclein decreases proteasome activity and increases sensitivity to mitochondria-dependent apoptosis, *Hum. Mol. Genet.* **10**, 919-926.
39. Giasson, B. I. and Duda, J. E. (2000) Oxidative damage linked to neurodegeneration by selective α -synuclein nitration in synucleinopathy lesions, *Science* **290**, 985.
40. Hashimoto, M., Hsu, L. J., Xia, Y., Takeda, A., Sisk, A., Sundsmo, M. and Masliah, E. (1999) Oxidative stress induces amyloid-like aggregate formation of NACP/ α -synuclein in vitro, *NeuroReport* **10**, 717-721.
41. Leroy, E., Boyer, R. and Polymeropoulos, M. H. (1998) Intron-exon structure of ubiquitin C-terminal hydrolase-L1, *DNA Research* **5**, 397-400.
42. Liu, Y., Fallon, L., Lashuel, H. A., Liu, Z. and Lansbury Jr, P. T. (2002) The UCH-L1 gene encodes two opposing enzymatic activities that affect α -synuclein degradation and Parkinson's disease susceptibility, *Cell* **111**, 209-218.
43. Zhang, Y., Gao, J., Chung, K. K. K., Huang, H., Dawson, V. L. and Dawson, T. M. (2000) Parkin functions as an E2-dependent ubiquitin-protein ligase and promotes the degradation of the synaptic vesicle-associated protein, CDCrel-1, *Proc. Natl. Acad. Sci. U. S. A.* **97**, 13354-13359.
44. Shimura, H., Hattori, N., Kubo, S.-I., Mizuno, Y., Asakawa, S., Minoshima, S., Shimizu, N., Iwai, K., Chiba, T., Tanaka, K. and Suzuki, T. (2000) Familial Parkinson disease gene product, parkin, is a ubiquitin-protein ligase, *Nat. Genet.* **25**, 302.
45. Imai, Y., Soda, M. and Takahashi, R. (2000) Parkin suppresses unfolded protein stress-induced cell death through its E3 ubiquitin-protein ligase activity, *J. Biol. Chem.* **275**, 35661-35664.
46. Ren, Y., Zhao, J. and Feng, J. (2003) Parkin binds to α / β tubulin and increases their ubiquitination and degradation, *J. Neurosci.* **23**, 3316-3324.

47. Jiang, H., Jiang, Q. and Feng, J. (2004) Parkin increases dopamine uptake by enhancing the cell surface expression of dopamine transporter, *J. Biol. Chem.* **279**, 54380-54386.
48. Shimura, H., Schwartz, D., Gygi, S. P. and Kosik, K. S. (2004) CHIP-Hsc70 complex ubiquitinates phosphorylated tau and enhances cell survival, *J. Biol. Chem.* **279**, 4869-4876.
49. Kim, S. J., Sung, J. Y., Um, J. W., Hattori, N., Mizuno, Y., Tanaka, K., Paik, S. R., Kim, J. and Chung, K. C. (2003) Parkin cleaves intracellular α -synuclein inclusions via the activation of calpain, *J. Biol. Chem.* **278**, 41890-41899.
50. Oluwatosin-Chigbu, Y., Robbins, A., Scott, C. W., Arriza, J. L., Reid, J. D. and Zysk, J. R. (2003) Parkin suppresses wild-type α -synuclein-induced toxicity in SHSY-5Y cells, *Biochem. Biophys. Res. Commun.* **309**, 679-684.
51. Chung, K. K. K., Zhang, Y., Lim, K. L., Tanaka, Y., Huang, H., Gao, J., Ross, C. A., Dawson, V. L. and Dawson, T. M. (2001) Parkin ubiquitinates the α -synuclein-interacting protein, synphilin-1: Implications for Lewy-body formation in Parkinson disease, *Nat. Med.* **7**, 1144-1150.
52. Marx, F. P., Holzmann, C., Strauss, K. M., Li, L., Eberhardt, O., Gerhardt, E., Cookson, M. R., Hernandez, D., Farrer, M. J., Kachergus, J., Engelender, S., Ross, C. A., Berger, K., Schols, L., Schulz, J. B., Riess, O. and Kruger, R. (2003) Identification and functional characterization of a novel R621C mutation in the synphilin-1 gene in Parkinson's disease, *Hum. Mol. Genet.* **12**, 1223-1231.
53. Hampshire, D. J., Roberts, E., Crow, Y., Bond, J., Mubaidin, A., Wriekat, A.-L., Al-Din, A. and Woods, C. G. (2001) Kufor-Rakeb syndrome, pallido-pyramidal degeneration with supranuclear upgaze paresis and dementia, maps to 1p36, *J. Med. Genet.* **38**, 680-682.
54. Aldin, A. S. N., Wriekat, A., Mubaidin, A., Dasouki, M. and Hiari, M. (1994) Pallido-pyramidal degeneration, supranuclear upgaze paresis and dementia - Kufor-Rakeb syndrome, *Acta Neurol. Scand.* **89**, 347-352.
55. Ramirez, A., Heimbach, A., Grundemann, J., Stiller, B., Hampshire, D., Cid, L. P., Goebel, I., Mubaidin, A. F., Wriekat, A.-L., Roeper, J., Al-Din,

- A., Hillmer, A. M., Karsak, M., Liss, B., Woods, C. G., Behrens, M. I. and Kubisch, C. (2006) Hereditary parkinsonism with dementia is caused by mutations in ATP13A2, encoding a lysosomal type 5 P-type ATPase, *Nat. Genet.* **38**, 1184(1188).
56. Lwin, A., Orvisky, E., Goker-Alpan, O., Lamarca, M. E. and Sidransky, E. (2004) Glucocerebrosidase mutation in subjects with parkinsonism, *Molec. Genet. Metab.* **81**, 70-73.
 57. Aharon-Peretz, J., Badarny, S., Rosenbaum, H. and Gershoni-Baruch, R. (2005) Mutations in the glucocerebrosidase gene and Parkinson disease: Phenotype-genotype correlation, *Neurology* **65**, 1460-1461.
 58. Pan, T., Kondo, S., Le, W. and Jankovic, J. (2008) The role of autophagy-lysosome pathway in neurodegeneration associated with Parkinson's disease, *Brain* **131**, 1969-1978.
 59. Valente, E. M., Brancati, F., Ferraris, A., Graham, E. A., Davis, M. B., Breteler, M. M. B., Gasser, T., Bonifati, V., Bentivoglio, A. R., De Michele, G., Dürr, A., Cortelli, P., Wassilowsky, D., Harhangi, B. S., Rawal, N., Caputo, V., Filla, A., Meco, G., Oostra, B. A., Brice, A., Albanese, A., Dallapiccola, B. and Wood, N. W. (2002) Park6-linked parkinsonism occurs in several European families, *Ann. Neurol.* **51**, 14-18.
 60. Wang, D., Qian, L., Xiong, H., Liu, J., Neckameyer, W. S., Oldham, S., Xia, K., Wang, J., Bodmer, R. and Zhang, Z. (2006) Antioxidants protect PINK1-dependent dopaminergic neurons in *Drosophila*, *Proc. Natl. Acad. Sci. U. S. A.* **103**, 13520-13525.
 61. Dodson, M. W. and Guo, M. (2007) Pink1, Parkin, DJ-1 and mitochondrial dysfunction in Parkinson's disease, *Curr. Opin. Neurobiol.* **17**, 331-337.
 62. Palacino, J. J., Sagi, D., Goldberg, M. S., Krauss, S., Motz, C., Wacker, M., Klose, J. and Shen, J. (2004) Mitochondrial dysfunction and oxidative damage in parkin-deficient mice, *J. Biol. Chem.* **279**, 18614-18622.
 63. Greene, J. C., Whitworth, A. J., Andrews, L. A., Parker, T. J. and Pallanck, L. J. (2005) Genetic and genomic studies of *Drosophila* parkin mutants implicate oxidative stress and innate immune responses in pathogenesis, *Hum. Mol. Genet.* **14**, 799-811.

64. Plun-Favreau, H., Klupsch, K., Moiso, N., Gandhi, S., Kjaer, S., Frith, D., Harvey, K., Deas, E., Harvey, R. J., McDonald, N., Wood, N. W., Martins, L. M. and Downward, J. (2007) The mitochondrial protease HtrA2 is regulated by Parkinson's disease-associated kinase PINK1., *Nat. Cell Biol.* **9**, 1243(1218).
65. Simon-Sanchez, J. and Singleton, A. B. (2008) Sequencing analysis of OMI/HTRA2 shows previously reported pathogenic mutations in neurologically normal controls, *Hum. Mol. Genet.* **17**, 1988-1993.
66. Ross, O. A., Soto, A. I., Vilariño-Güell, C., Heckman, M. G., Diehl, N. N., Hulihan, M. M., Aasly, J. O., Sando, S., Gibson, J. M., Lynch, T., Krygowska-Wajs, A., Opala, G., Barcikowska, M., Czyzewski, K., Uitti, R. J., Wszolek, Z. K. and Farrer, M. J. (2008) Genetic variation of Omi/HtrA2 and Parkinson's disease, *Parkinsonism Relat. Disord.* **14**, 539-543.
67. Martins, L. M., Morrison, A., Klupsch, K., Fedele, V., Moiso, N., Teismann, P., Abuin, A., Grau, E., Geppert, M., Livi, G. P., Creasy, C. L., Martin, A., Hargreaves, I., Heales, S. J., Okada, H., Brandner, S., Schulz, J. B., Mak, T. and Downward, J. (2004) Neuroprotective role of the reaper-related serine protease HtrA2/Omi revealed by targeted deletion in mice, *Mol. Cell Biol.* **24**, 9848-9862.
68. Jones, J. M., Datta, P., Srinivasula, S. M., Ji, W., Gupta, S., Zhang, Z., Davies, E., Hajnoczky, G., Saunders, T. L., Van Keuren, M. L., Fernandes-Alnemri, T., Meisler, M. H. and Alnemri, E. S. (2003) Loss of Omi mitochondrial protease activity causes the neuromuscular disorder of mnd2 mutant mice, *Nature* **425**, 721-727.
69. Van Duijn, C. M., Dekker, M. C. J., Bonifati, V., Galjaard, R. J., Houwing-Duistermaat, J. J., Snijders, P. J. L. M., Testers, L., Breedveld, G. J., Horstink, M., Sandkuijl, L. A., Van Swieten, J. C., Oostra, B. A. and Heutink, P. (2001) PARK7, a novel locus for autosomal recessive early-onset parkinsonism, on chromosome 1p36, *Am. J. Hum. Genet.* **69**, 629-634.
70. Taira, T., Saito, Y., Niki, T., Iguchi-Arigo, S. M. M., Takahashi, K. and Ariga, H. (2004) DJ-1 has a role in antioxidative stress to prevent cell death *EMBO Reports* **5**, 213-218.

71. Kim, R. H., Smith, P. D., Aleyasin, H., Hayley, S., Mount, M. P., Pownall, S., Wakeham, A., You-Ten, A. J., Kalia, S. K., Horne, P., Westaway, D., Lozano, A. M., Anisman, H., Park, D. S. and Mak, T. W. (2005) Hypersensitivity of DJ-1-deficient mice to 1-methyl-4-phenyl-1,2,3,6-tetrahydropyridine (MPTP) and oxidative stress, *Proc. Natl. Acad. Sci. U. S. A.* **102**, 5215-5220.
72. Weingarten, M. D., Lockwood, A. H., Hwo, S. Y. and Kirschner, M. W. (1975) A protein factor essential for microtubule assembly, *Proc. Natl. Acad. Sci. U. S. A.* **72**, 1858-1862.
73. Grundke-Iqbal, I., Iqbal, K., Quinlan, M., Tung, Y. C., Zaidi, M. S. and Wisniewski, H. M. (1986) Microtubule-associated protein tau a component of Alzheimer paired helical filaments, *J. Biol. Chem.* **261**, 6084-6089.
74. Grundke-Iqbal, I., Iqbal, K., Tung, Y. C., Quinlan, M., Wisniewski, H. M. and Binder, L. I. (1986) Abnormal phosphorylation of the microtubule-associated protein tau in Alzheimer cytoskeletal pathology, *Proc. Natl. Acad. Sci. U. S. A.* **83**, 4913-4917.
75. Iqbal, K., Zaidi, T., Wen, G. Y., Grundkeiqbal, I., Merz, P. A., Shaikh, S. S., Wisniewski, H. M., Alafuzoff, I. and Winblad, B. (1986) Defective brain microtubule assembly in Alzheimers-disease, *Lancet* **2**, 421-426.
76. Lee, V. M., Balin, B. J., Otvos, L., Jr. and Trojanowski, J. Q. (1991) A68: A major subunit of paired helical filaments and derivatized forms of normal tau, *Science* **251**, 675-678.
77. Arriagada, P. V., Growdon, J. H., Hedleywhyte, E. T. and Hyman, B. T. (1992) Neurofibrillary tangles but not senile plaques parallel duration and severity of Alzheimers-disease, *Neurology* **42**, 631-639.
78. Alonso, A. D. C., Li, B., Grundke-Iqbal, I. and Iqbal, K. (2006) Polymerization of hyperphosphorylated tau into filaments eliminates its inhibitory activity, *Proc. Natl. Acad. Sci. U. S. A.* **103**, 8864-8869.
79. Alonso, A. C., Zaidi, T., Grundke-Iqbal, I. and Iqbal, K. (1994) Role of abnormally phosphorylated tau in the breakdown of microtubules in Alzheimer disease, *Proc. Natl. Acad. Sci. U. S. A.* **91**, 5562-5566.

80. Li, B., Chohan, M., Grundke-Iqbal, I. and Iqbal, K. (2007) Disruption of microtubule network by Alzheimer abnormally hyperphosphorylated tau, *Acta Neuropathol.* **113**, 501-511.
81. Oliveira, S. A., Scott, W. K., Zhang, F. Y., Stajich, J. M., Fujiwara, K., Hauser, M., Scott, B. L., Pericak-Vance, M. A., Vance, J. M. and Martin, E. R. (2004) Linkage disequilibrium and haplotype tagging polymorphisms in the tau H1 haplotype, *Neurogenetics* **5**, 147-155.
82. Martin, E. R., Scott, W. K., Nance, M. A., Watts, R. L., Hubble, J. P., Koller, W. C., Lyons, K., Pahwa, R., Stern, M. B., Colcher, A., Hiner, B. C., Jankovic, J., Ondo, W. G., Allen, F. H., Jr., Goetz, C. G., Small, G. W., Masterman, D., Mastaglia, F., Laing, N. G., Stajich, J. M., Ribble, R. C., Booze, M. W., Rogala, A., Hauser, M. A., Zhang, F., Gibson, R. A., Middleton, L. T., Roses, A. D., Haines, J. L., Scott, B. L., Pericak-Vance, M. A. and Vance, J. M. (2001) Association of single-nucleotide polymorphisms of the tau gene with late-onset Parkinson disease, *JAMA* **286**, 2245-2250.
83. Coro Paisán-Ruíz, Nath, P., Washecka, N., Gibbs, J. R. and Singleton, A. B. (2008) Comprehensive analysis of LRRK2 in publicly available Parkinson's disease cases and neurologically normal controls, *Human Mutation* **29**, 485-490.
84. Berg, D., Schweitzer, K. J., Leitner, P., Zimprich, A., Lichtner, P., Belcredi, P., Brussel, T., Schulte, C., Maass, S., Nagele, T., Wszolek, Z. K. and Gasser, T. (2005) Type and frequency of mutations in the LRRK2 gene in familial and sporadic Parkinson's disease, *Brain* **128**, 3000-3011.
85. Paisán-Ruíz, C., Jain, S., Evans, E. W., Gilks, W. P., Simón, J., Van Der Brug, M., De Munain, A. L., Aparicio, S., Gil, A. M., Khan, N., Johnson, J., Martinez, J. R., Nicholl, D., Carrera, I. M., Pena, A. S., De Silva, R., Lees, A., Marti-Massó, J. F., Pérez-Tur, J., Wood, N. W. and Singleton, A. B. (2004) Cloning of the gene containing mutations that cause park8-linked Parkinson's disease, *Neuron* **44**, 595-600.
86. Goldberg, M. S., Pisani, A., Haburcak, M., Vortherms, T. A., Kitada, T., Costa, C., Tong, Y., Martella, G., Tscherter, A., Martins, A., Bernardi, G., Roth, B. L., Pothos, E. N., Calabresi, P. and Shen, J. (2005) Nigrostriatal dopaminergic deficits and hypokinesia caused by inactivation of the familial parkinsonism-linked gene DJ-1, *Neuron* **45**, 489-496.

87. Gloeckner, C. J., Kinkl, N., Schumacher, A., Braun, R. J., O'Neill, E., Meitinger, T., Kolch, W., Prokisch, H. and Ueffing, M. (2006) The Parkinson disease causing LRRK2 mutation I2020T is associated with increased kinase activity, *Neurosci. Lett.* **15**, 223-232.
88. Kachergus, J., Mata, I. F., Hulihan, M., Taylor, J. P., Lincoln, S., Aasly, J., Gibson, J. M., Ross, O. A., Lynch, T., Wiley, J., Payami, H., Nutt, J., Maraganore, D. M., Czyzewski, K., Styczynska, M., Wszolek, Z. K., Farrer, M. J. and Toft, M. (2005) Identification of a novel LRRK2 mutation linked to autosomal dominant parkinsonism: Evidence of a common founder across European populations, *Am. J. Hum. Genet.* **76**, 672-680.
89. Lang, A. E. and Lozano, A. M. (1998) Parkinson's disease - second of two parts, *N. Engl. J. Med.* **339**, 1130-1143.
90. Bower, J. H., Maraganore, D. M., McDonnell, S. K. and Rocca, W. A. (1999) Incidence and distribution of parkinsonism in Olmsted County, Minnesota, 1976-1990, *Neurology* **52**, 1214-1220.
91. Mayeux, R., Denaro, J., Hemenegildo, N., Marder, K., Tang, M.-X., Cote, L. J. and Stern, Y. (1992) A population-based investigation of Parkinson's disease with and without dementia: Relationship to age and gender, *Arch. Neurol.* **49**, 492-497.
92. Goetz, C. G., Tanner, C. M., Stebbins, G. T. and Buchman, A. S. (1988) Risk factors for progression in Parkinson's disease, *Neurology* **38**, 1841-1846.
93. Diamond, S. G., Markham, C. H., Hoehn, M. M., McDowell, F. H. and Muentner, M. D. (1989) Effect of age at onset on progression and mortality in Parkinson's disease, *Neurology* **39**, 1187-1190.
94. Hely, M. A., Morris, J. G. L., Reid, W. G. J., Osullivan, D. J., Williamson, P. M. and Broe, G. A. (1995) Age at onset: The major determinant of outcome in Parkinson's disease, *Acta Neurol. Scand.* **92**, 455-463.
95. Ozawa, T. (1995) Mitochondrial-DNA mutations associated with aging and degenerative diseases, *Exp. Gerontol.* **30**, 269-290.

96. Harley, C. B. (1991) Telomere loss - mitotic clock or genetic time bomb, *Mutat. Res.* **256**, 271-282.
97. Bjorksten, J. and Tenhu, H. (1990) The cross-linking theory of aging - added evidence, *Exp. Gerontol.* **25**, 91-95.
98. Beausejour, C. M., Krtolica, A., Galimi, F., Narita, M., Lowe, S. W., Yaswen, P. and Campisi, J. (2003) Reversal of human cellular senescence: Roles of the p53 and p16 pathways, *Embo J.* **22**, 4212-4222.
99. Kregel, K. C. and Zhang, H. J. (2007) An integrated view of oxidative stress in aging: Basic mechanisms, functional effects, and pathological considerations, *Am. J. Physiol.* **292**, R18-36.
100. Uversky, V. N. (2007) Neuropathology, biochemistry, and biophysics of α -synuclein aggregation, *J. Neurochem.* **103**, 17-37.
101. Schults, C. W. (2006) Lewy bodies, *Proc. Natl. Acad. Sci. U. S. A.* **103**, 1661-1668.
102. Lu, L., Neff, F., Alvarez-Fischer, D., Henze, C., Xie, Y., Oertel, W. H., Schlegel, J. R. and Hartmann, A. (2005) Gene expression profiling of Lewy body-bearing neurons in Parkinson's disease, *Exp. Neurol.* **195**, 27-39.
103. Bence, N. F., Sampat, R. M. and Kopito, R. R. (2001) Impairment of the ubiquitin-proteasome system by protein aggregation, *Science* **292**, 1552-1555.
104. Conway, K. A., Lee, S. J., Rochet, J. C., Ding, T. T., Williamson, R. E. and Lansbury, P. T., Jr. (2000) Acceleration of oligomerization, not fibrillization, is a shared property of both alpha-synuclein mutations linked to early-onset Parkinson's disease: Implications for pathogenesis and therapy, *Proc. Natl. Acad. Sci. U. S. A.* **97**, 571-576.
105. Volles, M. J. and Lansbury, P. T., Jr. (2002) Vesicle permeabilization by protofibrillar alpha-synuclein is sensitive to Parkinson's disease-linked mutations and occurs by a pore-like mechanism, *Biochemistry* **41**, 4595-4602.

106. Ding, T. T., Lee, S. J., Rochet, J. C. and Lansbury, P. T. (2002) Annular alpha-synuclein protofibrils are produced when spherical protofibrils are incubated in solution or bound to brain-derived membranes, *Biochemistry* **41**, 10209-10217.
107. Simakova, O. and Arispe, N. J. (2006) Early and late cytotoxic effects of external application of the Alzheimer's A β result from the initial formation and function of A β ion channels, *Biochemistry* **45**, 5907-5915.
108. Bucciantini, M., Giannoni, E., Chiti, F., Baroni, F., Formigli, L., Zurdo, J., Taddei, N., Ramponi, G., Dobson, C. M. and Stefani, M. (2002) Inherent toxicity of aggregates implies a common mechanism for protein misfolding diseases, *Nature* **416**, 507-511.
109. Duda, J. E., Giasson, B. I., Chen, Q. P., Gur, T. L., Hurtig, H. I., Stern, M. B., Gollomp, S. M., Ischiropoulos, H., Lee, V. M. Y. and Trojanowski, J. Q. (2000) Widespread nitration of pathological inclusions in neurodegenerative synucleinopathies, *Am. J. Path.* **157**, 1439-1445.
110. Pannathur, S., Jackson-Lewis, V., Przedborski, S. and Heinecke, J. W. (1999) Mass spectrometric quantification of 3-nitrotyrosine, ortho-tyrosine, and o,o'-dityrosine in brain tissue of 1-methyl-4-phenyl-1,2,3,6-tetrahydropyridine-treated mice, a model of oxidative stress in Parkinson's disease, *J. Biol. Chem.* **274**, 34621-34628.
111. Fink, A. L. (2006) The aggregation and fibrillation of α -synuclein, *Acc. Chem. Res.* **39**, 628-634.
112. Nielsen, L., Khurana, R., Coats, A., Frokjaer, S., Brange, J., Vyas, S., Uversky, V. N. and Fink, A. L. (2001) Effect of environmental factors on the kinetics of insulin fibril formation: Elucidation of the molecular mechanism, *Biochemistry* **40**, 6036-6046.
113. Lee, C. C., Nayak, A., Sethuraman, A., Belfort, G., Mcrae, G.J. (2007) A three-stage kinetic model of amyloid fibrillation *Biophys. J.* **92**, 3448-3458.
114. Shahi, P., Sharma, R., Sanger, S., Kumar, I., Jolly, R.S. (2007) Formation of amyloid fibrils via longitudinal growth of oligomers, *Biochemistry* **46**, 7365-7373.

115. Lomakin, A., Chung, D. S., Benedek, G. B., Kirschner, D. A. and Teplow, D. B. (1996) On the nucleation and growth of amyloid β protein fibrils: Detection of nuclei and quantitation of rate constants, *Proc. Natl. Acad. Sci. U. S. A.* **93**, 1125-1129.
116. LeVine, H. (1999) Quantification of β -sheet amyloid fibril structures with thioflavin T, *Method. Enzymol.* **309**, 274-284.
117. Uversky, V. N., Lee, H. J., Li, J., Fink, A. L. and Lee, S. J. (2001) Stabilization of partially folded conformation during alpha synuclein oligomerization in both purified and cytosolic preparations, *J. Biol. Chem.* **276**, 43495-43498.
118. Atwood, C. S., Perry, G., Zeng, H., Kato, Y., Jones, W. D., Ling, K., Huang, X., Moir, R. D., Wang, D., Sayre, L. M., Smith, M. A., Chen, S. G. and Bush, A. I. (2004) Copper mediates dityrosine cross-linking of Alzheimer's amyloid beta, *Biochemistry* **43**, 560-568.
119. Norris, E. H., Giasson, B. I., Ischiropoulos, H. and Lee, V. M. (2003) Effects of oxidative and nitrative challenges on α -synuclein fibrillogenesis involve distinct mechanisms of protein modifications, *J. Biol. Chem.* **278**, 27230-27240.
120. Hashimoto, M., Takeda, A., Hsu, L. J., Takenouchi, T. and Masliah, E. (1999) Role of cytochrome c as a stimulator of alpha-synuclein aggregation in Lewy body disease, *J. Biol. Chem.* **274**, 28849-28852.
121. Shigenaga, M. K., Hagen, T. M. and Ames, B. N. (1994) Oxidative damage and mitochondrial decay in aging, *Proc. Natl. Acad. Sci. U. S. A.* **91**, 10771-10778.
122. Lashuel, H. A., Hartley, D., Petre, B. M., Walz, T. and Lansbury, P. T., Jr. (2002) Amyloid pores from pathogenic mutations, *Nature* **418**, 291.
123. Olteanu, A. and Pielak, G. J. (2004) Peroxidative aggregation of α -synuclein requires tyrosines, *Protein Sci.* **13**, 2852-2856.
124. Barr, D. P., Gunther, M. R., Deterding, L. J., Tomer, K. B. and Mason, R. P. (1996) ESR spin-trapping of a protein-derived tyrosyl radical from the

- reaction of cytochrome c with hydrogen peroxide, *J. Biol. Chem.* **271**, 15498-15503.
125. Deterding, L. J., Barr, D. P., Mason, R. P. and Tomer, K. B. (1998) Characterization of cytochrome c free radical reaction with peptides by mass spectrometry, *J. Biol. Chem.* **273**, 12963-112869.
 126. Brooks, A. I., Chadwick, C. A., Gelbard, H. A., Cory-Slechta, D. A. and Federoff, H. J. (1999) Paraquat elicited neurobehavioral syndrome caused by dopaminergic neuron loss, *Brain Res.* **823**, 1-10.
 127. Manning-Bog, A. B., McCormack, A. L., Li, J., Uversky, V. N., Fink, A. L. and Di Monte, D. A. (2002) The herbicide paraquat causes up-regulation and aggregation of α -synuclein in mice., *J. Biol. Chem.* **277**, 1641-1644.
 128. Sherer, T. B., Kim, J.-H., Betarbet, R. and Greenamyre, J. T. (2003) Subcutaneous rotenone exposure causes highly selective dopaminergic degeneration and α -synuclein aggregation, *Exp. Neurol.* **179**, 9-16.
 129. Betarbet, R., Sherer, T. B., Mackenzie, G., Garcia-Osuna, M., Panov, A. V. and Greenamyre, J. T. (2000) Chronic systemic pesticide exposure reproduces features of Parkinson's disease, *Nat. Neurosci.* **3**, 1301-1306.
 130. Sakka, N., Sawada, H., Izumi, Y., Kume, T., Katsuki, H., Kaneko, S., Shimohama, S. and Akaike, A. (2003) Dopamine is involved in selectivity of dopaminergic neuronal death by rotenone, *NeuroReport* **14**, 2425-2428.
 131. Sanchez-Ramos, J., Facca, A., Basit, A. and Song, S. (1998) Toxicity of dieldrin for dopaminergic neurons in mesencephalic cultures, *Exp. Neurol.* **150**, 263-271.
 132. Uversky, V. N., Li, J. and Fink, A. L. (2001) Pesticides directly accelerate the rate of alpha synuclein fibril formation: A possible factor in Parkinson's disease, *FEBS Lett.* **500**, 105-108.
 133. Sun, F., Anantharam, V., Latchoumycandane, C., Kanthasamy, A. and Kanthasamy, A. G. (2005) Dieldrin induces ubiquitin-proteasome dysfunction in α -synuclein overexpressing dopaminergic neuronal cells and enhances susceptibility to apoptotic cell death, *J. Pharmacol. Exp. Ther.* **315**, 69-79.

134. Morato, G. S., Lemos, T. and Takahashi, R. N. (1989) Acute exposure to maneb alters some behavioral functions in the mouse, *Neurotoxicol. Teratol.* **11**, 421-425.

Chapter 2 Gene Construction and Protein Expression, Purification, and Fluorescent Labeling of Wild-Type and Variant Recombinant Human α -Synuclein and Cytochrome c

Reproduced in part with permission from *Biochemistry*. Copyright 2008 American Chemical Society

2.1 Introduction

Western blot antibody staining has traditionally been used to detect α -synuclein covalent aggregation (1-4). This technique, however, has several limitations. First, proteins must be transferred from the poly-acrylamide gel into a nitrocellulose or polyvinylidene fluoride membrane. Because the α -synuclein aggregation reaction encompasses protein species from 12 to over 200 kDa, different transfer conditions must be used for different areas of the gel. This situation often leads to inconsistencies in the appearance of the protein bands in the two halves of the transfer. Second, the primary antibodies may not recognize all covalently aggregated species with the same sensitivity, leading to a disconnection between the intensity and the amount of protein aggregate in each band. Last, both α -synuclein and cytochrome c are used in the covalent aggregation reaction and both proteins be monitored. Since antibody staining

does not allow simultaneous visualization of the two proteins, the membrane must be probed for α -synuclein, stripped, and re-probed for cytochrome *c*. This process can take up to four days. To overcome these obstacles, I developed a method for fluorescently labeling each protein before the covalent aggregation process. This allows both proteins to be visualized in the polyacrylamide gel, maintains the correlation between band intensity and amount of protein, and facilitates the completion of multiple experiments within a single day.

2.2 Materials and Methods

2.2.1 Preparation of Mutant Recombinant Human α -Synucleins and Cytochrome *c*

The wild-type α -synuclein (5), human cytochrome *c* (6) and the no-tyrosine α -synuclein mutant (1) were used as described. Twenty-five additional human α -synuclein mutants in the pT7-7 vector were created by using a site-directed mutagenesis kit (QuickChange, Stratagene, La Jolla, CA). Mutants with one, two, or three tyrosine codons converted to phenylalanine codons were created with the following forward primers from the Nucleic Acid Core Facility in the UNC Lineberger Cancer Center (nucleotide changes are underlined):

Y39F unknown

Y125F 5' CCTGACAATGAGGCTTTTGAAATGCCTTCTGAG 3'

Y133F 5' CTTCTGAGGAAGGGTTTCAAGACTACGAACC 3'

Y136F 5' GCCTTCTGAGGAAGGGTACCAAGACTTCGAACCTG
AAGCCTAAC 3'

Y133F,Y136F 5' CTTCTGAGGAAGGGTTTCAAGACTTCGAAC 3'

Valine-to-cysteine mutations were introduced in the wild-type α -synuclein construct, the tyrosine-combination mutants, and the wild-type human cytochrome *c* construct for labeling purposes. Using the following forward primers, all α -synucleins had valine 3 mutated to cysteine, and an additional wild-type construct was generated with valine 66 mutated to cysteine:

V3C 5' GGAGATATACATATGGATTTGCTTTCATGAAAGGACTTTCAA 3'

V66C 5' CAAAGAGCAAGTGACAAATTGCGGAGGAGCAGTGGTGACG 3'

Using the following forward primer, the wild-type human cytochrome *c* construct had lysine 39 mutated to cysteine:

K39C 5' CTGTTTCGGCCGCTTGCACGGGCCAGGC 3'

All nucleotide sequences were confirmed by the UNC Automated DNA Sequencing Facility.

2.2.2 Growth, Purification, and Storage of Wild-Type and Variant Recombinant Human α -Synucleins and Cytochromes *c*

Wild-type and mutant α -synucleins were transformed into BL21 *E. coli* (Invitrogen, Carlsbad, CA). A single colony was used to inoculate 20 mL of Miller Luria Broth (Fisher Scientific, Fair Lawn, NJ) supplemented with 100 mg•L⁻¹ ampicillin (LB_{amp}), and the resulting culture was grown at 37°C with shaking overnight. The overnight culture was used to inoculate an additional 1L of LB_{amp}, which was then grown at 37°C with shaking until it reached an optical density at 600 nm (O.D.₆₀₀) of 0.6-0.8. The culture was then induced with isopropyl β -D-1-

thiogalactopyranoside (IPTG) to a final concentration of 1 mM. After 4 h, the cells were harvested via centrifugation at 4,500 g for 30 min and stored at -20°C.

The cells were resuspended in 20 mL of lysis buffer per liter of culture (20-mM Tris, pH 8.0; 1-mM ethylenediamine-tetraacetic acid [EDTA]; 1-mM phenyl-methylsulphonyl fluoride [PMSF, Pierce, Rockford, IL]; 1-mM dithiothreitol [DTT, only for V3C or V66C variants]). After sonication (Sonic Dismemberator, Fisher Scientific, Fair Lawn, NJ) for 5 min at a 70% duty cycle, the cells were boiled for 30 min then centrifuged at 20,200 g for 30 min. For the V3C or V66C variants, the resulting supernatant was supplemented with DTT to a final concentration of 1M. All variants were subjected to a $10 \text{ g} \bullet \text{L}^{-1}$ streptomycin sulfate cut to precipitate nucleic acids then centrifuged at 20,200 g for 30 min. The resulting supernatant was subjected to a $361 \text{ g} \bullet \text{L}^{-1}$ $(\text{NH}_4)_2\text{SO}_4$ cut to precipitate α -synuclein then centrifuged at 20,200 g for 30 min. The protein pellet was resuspended in 20 mL of buffer (20-mM Tris, pH 8.0, 1-mM DTT [only for V3C or V66C variants]) and dialyzed (SnakeSkin, 10,000 MWCO, Pierce) into 2 L of the same buffer at 4°C overnight. The protein was further purified via chromatography using a HiLoad 16/10 Q Sepharose High Performance column (GE Healthcare, Uppsala, Sweden) in dialysis buffer with a linear gradient from 0-M to 1-M NaCl. Fractions containing pure α -synuclein (as determined by Coomassie-stained sodium dodecyl sulfate polyacrylamide gel electrophoresis [SDS-PAGE]) were combined and dialyzed (SnakeSkin, 10,000 MWCO) into water at 4°C overnight. The protein concentration was determined with the Lowry method (7) (Modified Lowry Protein Assay Kit, Pierce) with human

recombinant cytochrome *c* (6) as a standard. After purification, proteins were aliquoted and lyophilized for storage at -80°C.

Wild-type and mutant cytochromes *c* were transformed into BL21 *E. coli*. A single colony was used to inoculate 50 mL of terrific broth (12 g•L⁻¹ tryptone, 24 g•L⁻¹ yeast extract, 5% glycerol, 12.6 g•L⁻¹ KH₂PO₄, 2.3 g•L⁻¹ K₂HPO₄) supplemented with 100 mg•L⁻¹ ampicillin (TB_{amp}). The resulting culture was grown at 37°C with shaking overnight. The overnight culture was used to inoculate an additional 1L of TB_{amp}, which was then grown at 37°C with shaking for 24 - 48 h. The cells were harvested via centrifugation at 4,500 g.

The cells were resuspended in 20 mL of lysis buffer per liter of culture (20-mM NaH₂PO₄, pH 7.4; 1-mM EDTA; 1-mM PMSF; 1-mM DTT [K39C variant only]). After four rounds of sonication for 5 min at a 50% duty cycle, the cells were centrifuged at 20,200 g for 30 min. The resulting supernatant was subjected to a 10 g•L⁻¹ streptomycin sulfate cut to precipitate nucleic acids then centrifuged at 20,200 g for 30 min. The resulting supernatant was subjected to a 350 g•L⁻¹ (NH₄)₂SO₄ cut to precipitate unwanted proteins then centrifuged at 20,200 g for 30 min. The cytochrome *c* supernatant was dialyzed (SnakeSkin, 10,000 MWCO) into 10 L of water (with 1-mM DTT for K39C variant) at 4°C overnight. The protein was further purified via chromatography using a HiLoad 16/10 SP Sepharose High Performance column (GE Healthcare) in buffer (20-mM NaH₂PO₄, pH 7.4; 1-mM DTT [K39C variant only]) with a linear gradient from 0-M to 1-M NaCl. Fractions containing pure cytochrome *c* (as determined by Coomassie-stained SDS-PAGE) were combined and dialyzed (SnakeSkin,

10,000 MWCO) into water at 4°C overnight. Protein concentration was determined from the absorbance at 410 nm by using a molar extinction coefficient of $106.1 \text{ mM}^{-1}\bullet\text{cm}^{-1}$ (8). After purification, proteins were aliquoted and lyophilized for storage at -80°C.

2.2.3 Alexa Fluor Labeling of Wild-Type and Variant Recombinant

Human α -Synucleins and Cytochrome c

Sixty nmol of V3C or V66C α -synuclein were reacted with 300 nmol of Alexa Fluor 633 C₅ maleimide (Invitrogen) in 20-mM Tris, pH 7.5 for 2 h at room temperature and then at 4°C for 18-66 h. Unreacted cysteines were blocked with 3 mmol of iodoacetamide (IAA). Unreacted dye was removed with a two-step chromatography process. First, the bulk of the free dye was removed using a HiTrap desalting column (GE Healthcare) in 20-mM phosphate buffer, pH 7.4, containing 150-mM NaCl and 15% v/v acetonitrile. A subsequent, more rigorous, purification was performed by using a Superdex200 10/300 column (GE Healthcare) in the same buffer. Fractions with no remaining unreacted dye as determined by SDS-PAGE were dialyzed (7000 MWCO cassette, Pierce) into water, aliquoted and lyophilized for storage at -80°C.

The K39C variant of cytochrome c was labeled by using Alexa Fluor 488 C₅ maleimide (Invitrogen) and purified in the same way, except that the second chromatography step was not required.

2.2.4 Fibril Growth

α -Synuclein (200- μ M of the pure or a 9:1 mole:mole mixture of pure and Alexa Fluor 633 labeled protein) in 20-mM phosphate buffer (pH 7.4), 150-mM

NaCl, and 1-mM EDTA was shaken at 37°C and 225 rpm for 48 h. Fibril growth was quantified via thioflavin-T fluorescence in a 96-well plate using the VersaDoc MP imager. Fibrils were separated from α -synuclein monomers and smaller aggregates by centrifugation at 17,000 g for 10 min. Total protein concentration of the resulting supernatant was determined via the Lowry method. The amount of Alexa Fluor 633 was determined via absorbance at 655 nm using a molar extinction coefficient of 72,000 M⁻¹cm⁻¹ (9).

2.3 Results and Discussion

2.3.1 Purification of α -Synuclein Labeled with Alexa Fluor Requires a Multi-Step Approach.

Initial attempts at removing free Alexa Fluor from the reaction mixture using dialysis, as suggested by the manufacturer, resulted in calculated labeling ratios of greater than 100%. To determine if the excess Alexa Fluor was attaching to α -synuclein in a covalent or non-covalent manner, MALDI/MS was employed. This technique was chosen because it can detect Alexa Fluor that is covalently attached to α -synuclein, and gives an estimate of the extent of labeling by comparing the peak intensities of the unlabeled and labeled protein. As shown in Figure 2.1, only one Alexa Fluor molecule is covalently attached to each α -synuclein, and not all of the α -synuclein molecules are labeled with dye. This indicated that the excess Alexa Fluor was binding to the α -synuclein in a non-covalent manner. Although the manufacturer does not provide the structure of Alexa Fluor 633, as seen by the structure of Alexa Fluor 488 (Figure 2.2), all of the Alexa Fluor dyes share a similar head-group that contains both aromatic and

charged regions. Since α -synuclein has hydrophobic and charged regions that are not protected by secondary structure, it is likely that the dye associates with the protein via hydrophobic interactions, electrostatic interactions, or both. To overcome these interactions, the buffer for chromatographic purification was changed from water to phosphate-buffered saline with 15% acetonitrile. Also, because such a large excess of dye is required to produce a significant degree of labeling, an additional gel-filtration step was added after desalting. These changes yielded a labeling efficiency of 45.0% for the WT:V66C variant (Table 2.1), which agrees with the calculated ratio from the MS peak intensity data of 50%. While labeling efficiencies vary greatly between the variants, the differences reflect the batch in which the protein was labeled, not any inherent differences in the variants. Because the labeled protein only made up approximately 10% of the total α -synuclein, labeling efficiencies over 10% were deemed acceptable for further use.

2.3.2 Position of Alexa Fluor 633 on α -Synuclein does Not Affect α -Synuclein Behavior.

Wild-type α -synuclein was created with Alexa Fluor attached at either cysteine 3 or cysteine 66 to ensure that the position of the Alexa Fluor dye did not affect the behavior of the protein in oxidative aggregation reactions (see Chapter 3). These sites were chosen because they are in highly dynamic regions of the protein (10) (which decreases the possibility that labeling might disrupt native conformation). As seen in Figure 2.4, regardless of Alexa Fluor position, both cytochrome *c* and H_2O_2 are required for tyrosine-dependant α -

synuclein aggregation, and both α -synuclein variants exhibit the same aggregation pattern.

Since position 66 is in the core needed for fibril formation (11), position 3 was chosen for all subsequent studies. As seen in Figure 2.5, the fibril pellet of unlabeled α -synuclein is white, and the fibril pellet of Alexa Fluor 633 labeled α -synuclein is blue, indicating that the labeled protein is capable of achieving the conformation needed for fibril formation. Additionally, the unlabeled:labeled ratio of protein that was not incorporated into the fibrils was 9:1, the same as the initial ratio. These observations indicate that the Alexa Fluor labeled protein is neither preferentially included nor excluded from the fibrils, compared to the unlabeled protein.

2.3.3 Alexa Fluor 488 Only Labels Cytochrome c at the Added Cys39, Not at the Endogenous Cys14 or Cys17.

Human cytochrome c contains two endogenous cysteine residues at positions 14 and 17, which are covalently attached to the heme. An additional cysteine was introduced at position 39 to facilitate Alexa Fluor binding. This site was chosen because the analogous site in yeast cytochrome c has been used successfully to label the protein with exogenous molecules without affecting the structure or function of the protein (12). To confirm that the Alexa Fluor reacted exclusively with cysteine 39, MALDI/MS was employed following tryptic digestion of the protein. As seen in Figure 2.6, the cysteine-containing fragments (residues 14-22 and 39-55) are visible in the unlabeled protein sample. As expected, the 39-55 fragment is barely detectable in the labeled protein sample,

while a peak corresponding to the 39-55 fragment bound with Alexa Fluor 488 is visible. Also, no peak is detected for the mass of the 14-22 fragment bound to Alexa Fluor 488.

2.4 Conclusions

Labeling proteins with Alexa Fluor maleimide dye is an excellent way to monitor proteins in a variety of biological and biochemical experiments. Since cysteine is the second-to-least often used amino acid in proteins (13), it is possible to singly-label a wide range of proteins, either using an endogenous cysteine or by introducing one via site-directed mutagenesis. The dyes come in a range of colors, allowing the simultaneous monitoring of several proteins in a single setting. Although labeling efficiencies depend on reaction conditions, adjustment of reaction parameters and the specific dye used can provide labeling efficiencies over 80%, which are sufficient for most biological and biochemical experiments. Lastly, a single sample of dye-labeled protein can be analyzed with multiple techniques or used in multiple types of experiments, which can greatly accelerate method development and data acquisition.

2.5 Figures and Tables

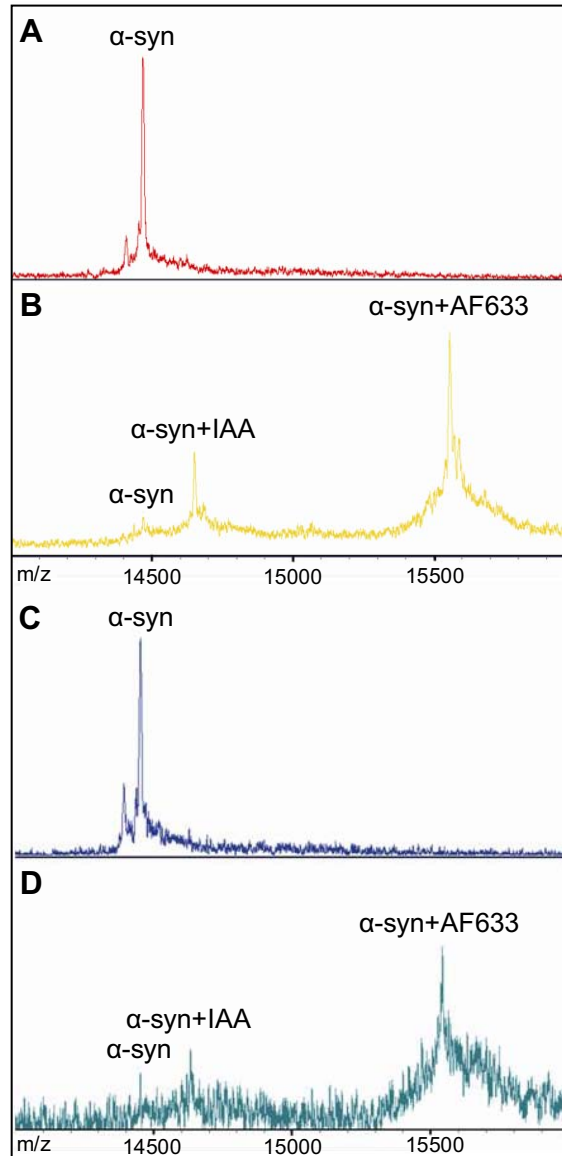


Figure 2.1 MALDI/MS of α -synuclein with or without Alexa Fluor 633 label.

Panel A: WT:V66C. The mass peak of the unmodified protein is indicated.

Panel B: WT:V66C labeled with Alexa Fluor 633. Mass shifts representing the binding of iodoacetamide (+~180) or Alexa Fluor 633 (+~1100) to the protein are indicated. **Panel C:** Y133F:V3C. The mass peak of the unmodified protein is indicated. **Panel D:** Y133F:V3C labeled with Alexa Fluor 633. Mass shifts representing the binding of iodoacetamide (+~180) or Alexa Fluor 633 (+~1100) to the protein are indicated.

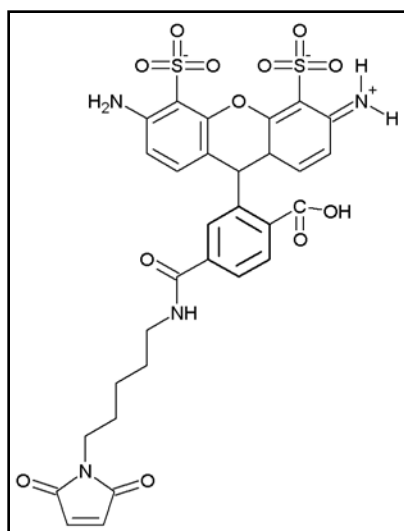


Figure 2.2 Structure of Alexa Fluor 488 C₅ maleimide.

Variant	Labeling Efficiency
WT:V3C	56.3%
WT:V66C	45.0%
Y39F	39.4%
Y125F	36.1%
Y133F	31.4%
Y136F	37.3%
39/125 only	13.4%
39/133 only	13.9%
39/136 only	11.6%
39 only	98.6%
125 only	58.5%
133 only	88.7%
136 only	87.3%
noY	~50%

Table 2.1 Labeling efficiencies of α -synuclein with Alexa Fluor 633.

Efficiencies were calculated by dividing total Alexa Fluor concentration (as determined by absorbance at 655 nm, using a molar extinction coefficient of $72,000 \text{ M}^{-1}\text{cm}^{-1}$) by total α -synuclein concentration (as determined by the Lowry method, see Materials and Methods).

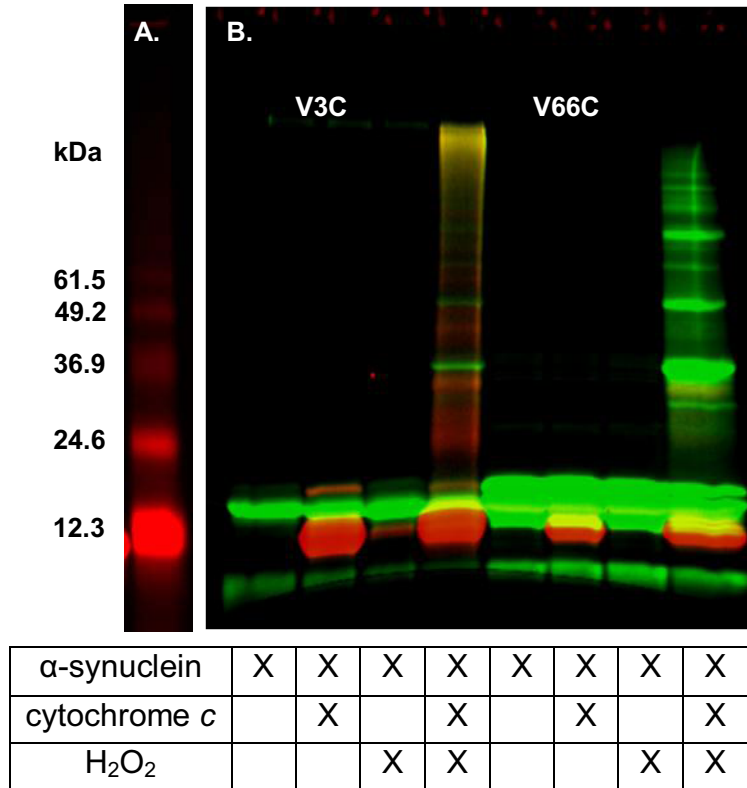


Figure 2.3 Position of Alexa Fluor tag does not affect covalent aggregation.
Panel A: Cytochrome c was incubated with H₂O₂ to form a molecular weight marker. **Panel B:** Wild-type α-synuclein, with the Alexa Fluor label at position 3 (V3C, lanes 1-4), or at position 66 (V66C, lanes 5-8) were combined with various combinations of cytochrome c and H₂O₂ for 90 min., separated on a 10-20% gradient polyacrylamide gel, and visualized by fluorescence (green, α-synuclein; red, cytochrome c).

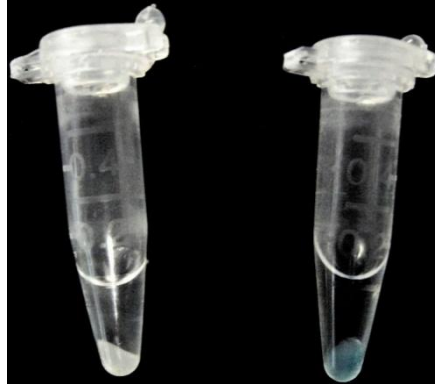


Figure 2.4 Alexa Fluor 633 labeled α -synuclein is capable of forming fibrils.
Left Tube: fibrils grown from only unlabeled WT α -synuclein. **Right Tube:** Fibrils grown from 90% unlabeled WT α -synuclein and 10% WT:V3C α -synuclein labeled with Alexa Fluor 633

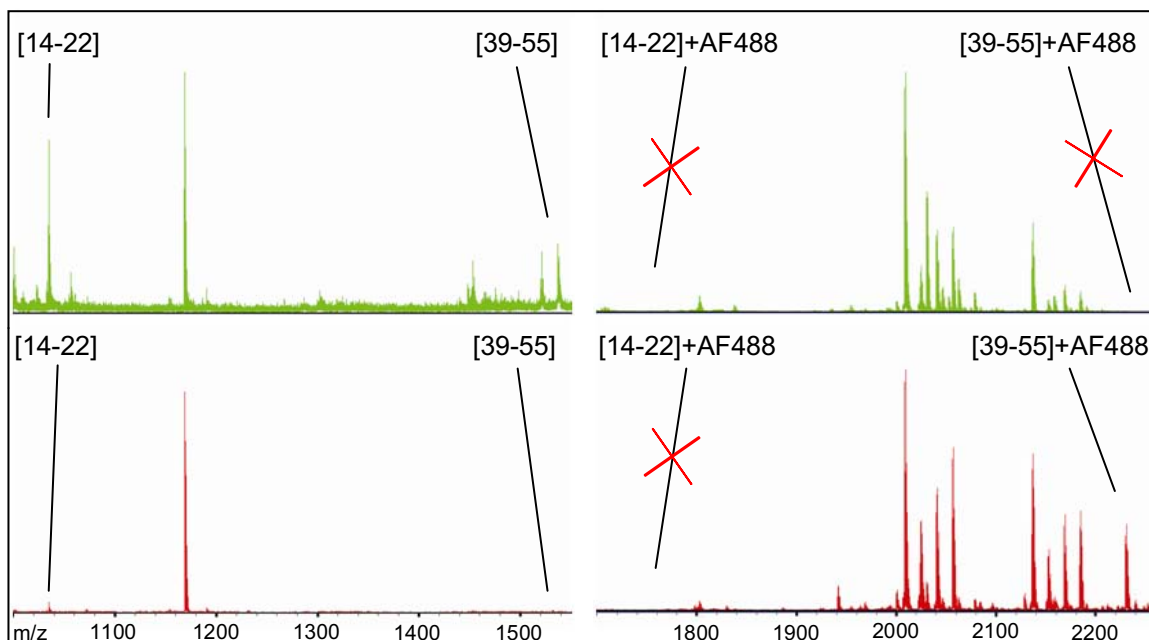


Figure 2.5 MALDI/MS of cytochrome c with or without Alexa Fluor 488 label.

Top Panel: K39C cytochrome c. Both cysteine-containing tryptic peptides are identifiable, but no masses corresponding to Alexa Fluor-bound peptides are detected. **Bottom Panel:** K39C cytochrome c labeled with Alexa Fluor 488. Alexa Fluor 488 is only found bound to the correct peptide (39-55 fragment).

2.6 References

1. Olteanu, A. and Pielak, G. J. (2004) Peroxidative aggregation of α -synuclein requires tyrosines, *Protein Sci.* **13**, 2852-2856.
2. Souza, J. M., Giasson, B. I., Chen, Q., Lee, V. M. and Ischiropoulos, H. (2000) Dityrosine cross-linking promotes formation of stable alpha - synuclein polymers. Implication of nitrative and oxidative stress in the pathogenesis of neurodegenerative synucleinopathies, *J. Biol. Chem.* **275**, 18344-18349.
3. Norris, E. H., Giasson, B. I., Ischiropoulos, H. and Lee, V. M. (2003) Effects of oxidative and nitrative challenges on α -synuclein fibrillogenesis involve distinct mechanisms of protein modifications, *J. Biol. Chem.* **278**, 27230-27240.
4. Takahashi, T., Yamashita, H., Nakamura, T., Nagano, Y. and Nakamura, S. (2002) Tyrosine 125 of α -synuclein plays a critical role for dimerization following nitrative stress, *Brain Res.* **938**, 73-80.
5. McNulty, B. C., Tripathy, A., Young, G. B., Orans, J. and Pielak, G. J. (2005) Temperature-induced reversible conformational change in the first 100 residues of alpha-synuclein, *Protein Sci.* **15**, 602-608.
6. Olteanu, A., Patel, C. N., Dedmon, M. M., Kennedy, S., Linhoff, M. W., Minder, C. M., Potts, P. R., Deshmukh, M. and Pielak, G. J. (2003) Stability and apoptotic activity of recombinant human cytochrome c, *Biochem. Biophys. Res. Commun.* **312**, 733-740.
7. Lowry, O. H., Rosebrough, N. J., Farr, A. L. and Randall, R. J. (1951) Protein measurement with the Folin phenol reagent, *J. Biol. Chem.* **193**, 265-275.
8. Margoliash, E. and Frohwirt, N. (1959) Spectrum of horse-heart cytochrome c, *Biochem. J.* **71**, 570-572.
9. www.invitrogen.com
10. Bertoncini, C. W., Jung, Y. S., Fernandez, C. O., Hoyer, W., Greisinger, C., Jovin, T. M. and Zweckstetter, M. (2005) Release of long range tertiary

- interactions potentiates aggregation of natively unstructured alpha-synuclein, *Proc. Natl. Acad. Sci. U. S. A.* **102**, 1430-1435.
11. Vilar, M., Chou, H.-T., Luhrs, T., Maji, S. K., Riek-Loher, D., Verel, R., Manning, G., Stahlberg, H. and Riek, R. (2008) The fold of α -synuclein fibrils, *Proc. Natl. Acad. Sci. U. S. A.* **105**, 8637-8642.
 12. Geren, L. M., Beasley, J. R., Fine, B. R., Saunders, A. J., Hibdon, S., Pielak, G. J., Durham, B. and Millett, F. (1995) Design of a ruthenium-cytochrome *c* derivative to measure electron transfer to the initial acceptor in cytochrome *c* oxidase, *J. Biol. Chem.* **270**, 2466-2472.
 13. Creighton, T. E. (1993) *Proteins*, Second, W.H. Freeman and Company, New York.

Chapter 3 α -Synuclein Conformation Affects its Tyrosine-Dependent Oxidative Aggregation

Reproduced in part with permission from *Biochemistry*. Copyright 2008 American Chemical Society

3.1 Introduction

As discussed in Chapter 1, oxidative stress and the aggregation of α -synuclein are critical components of Parkinson's disease. To study the interplay between these two processes, it is essential to choose the proper oxidation system. It must produce tyrosine-dependant covalent aggregation of α -synuclein and include components that could come in contact with α -synuclein in cells. Based on these criteria, I have chosen the cytochrome *c*/H₂O₂, also called the peroxidative, system. Our lab has previously shown that the peroxidative system causes tyrosine-dependent covalent aggregation of α -synuclein (1), and in times of oxidative stress is it possible that cytochrome *c* and H₂O₂ can leak into the cytosol (2) aided by pores in the mitochondrial membrane formed by α -synuclein (3). To monitor the behavior of α -synuclein in the peroxidative system, I have developed a method of fluorescently labeling and purifying α -synuclein and the labeled cytochrome *c*, which allows simultaneous monitoring of both proteins.

Here, I shed light on the process of both peroxidative and non-covalent aggregation of α -synuclein and how these forms of aggregation may be related.

Specifically, I address the role of each tyrosine residue and show how the protein's conformation affects covalent aggregation.

3.2 Materials and Methods

3.2.1 Covalent Aggregation Assays

α -Synuclein (100 μ M, 9:1 unlabeled:Alexa Fluor labeled for wild-type), cytochrome *c* (10 μ M, 1:3 unlabeled:Alexa Fluor labeled) and H_2O_2 (10 mM) were reacted in phosphate-buffered saline (PBS: 20-mM Na_2HPO_4 , pH 7.4, 150-mM NaCl) at 37°C for 90 min. To compensate for the varying Alexa Fluor labeling efficiencies of α -synuclein variants, the amount of labeled α -synuclein was adjusted so that each variant had the same total fluorescence as the wild-type control sample. Control experiments show that this adjustment does not affect the conclusions. For the cytochrome *c* control reaction, 100- μ M cytochrome *c* (100% Alexa Fluor labeled) and 10-mM H_2O_2 were reacted under the same conditions as above. Samples were resolved by electrophoresis on 10-20% gradient sodium dodecyl sulfate (SDS) polyacrylamide gels (PAG) (Criterion, BioRad) for 75 min at 200 V. Gels were analyzed for fluorescence with a VersaDoc MP imager (BioRad) and for total protein content with Coomassie Blue staining.

3.2.2 Fibril Formation

α -Synuclein (200 μ M) in PBS with 1-mM EDTA was shaken at 37°C and 225 rpm for 48 h. Fibril growth was quantified via thioflavin-T fluorescence in a 96-well plate by using the VersaDoc MP imager. Cytochrome *c* (final concentration 20 μ M) and H_2O_2 (final concentration 20 mM) were added to the

reaction either at the beginning or at the end of the shaking period. Fibrils were separated from α -synuclein monomers and smaller aggregates by centrifugation at 1.7×10^4 g for 10 min. Fibrils (pellet) and small aggregates (supernatant) were treated with SDS and boiled for 10 min before being analyzed by SDS-PAGE as described above.

3.3 Results

3.3.1 Alexa Fluor Labeling and Tyrosine-Dependent α -Synuclein Covalent Aggregation.

The wild-type protein and the variant containing no tyrosines were combined with cytochrome *c* and H_2O_2 . Figure 3.1A shows the results of the reaction between cytochrome *c* and H_2O_2 as a standard. As shown in Figure 3.1B, cytochrome *c* and H_2O_2 , as well as the tyrosines in α -synuclein, are required for oxidative aggregation. This result agrees with our previous work, which used Coomassie Blue and anti- α -synuclein antibody detection (1). In all peroxidative aggregation reactions, a population of α -synuclein monomer is left unreacted, even after exposure to additional cytochrome *c* and H_2O_2 . This result indicates that some portion of the α -synuclein is rendered incapable of covalent aggregation after exposure to cytochrome *c* and H_2O_2 . This effect has also been seen when human neuroglobin is exposed to peroxide (4). Alexa Fluor labels on α -synuclein and cytochrome *c* allow facile detection of peroxidative covalent aggregation of α -synuclein.

3.2.2 Reactivity of the Tyrosines in α -Synuclein to Covalent Aggregation.

To examine the chemical reactivity of each tyrosine, four variants, each containing only one tyrosine, were reacted with cytochrome *c* and H₂O₂. Our conditions do not promote non-covalent aggregation of α -synuclein. Figure 3.2A shows the reaction between cytochrome *c* and H₂O₂ as a standard. Figure 3.2B shows the differing ability of each tyrosine to form inter-molecular dityrosine bonds. Tyrosines 133 and 136 are the most reactive, as shown by distinct dimer formation and little α -synuclein degradation. Streaking of the α -synuclein because of random backbone cleavage and large amounts of degraded α -synuclein indicate that tyrosine 125 is less able to accept a radical from cytochrome *c*. Lack of α -synuclein dimer and large amounts of degradation indicate that tyrosine 39 is the least reactive. Tyrosine 39 is so unreactive that it does not form an intact heterodimer with cytochrome *c* as seen in the other variants. Instead, some of the free radicals generated cause degradation of the heterodimer. In summary, the chemical reactivities of the tyrosines in α -synuclein to form dityrosines increase in the following order: 39, 125, 133/136.

3.2.3 Tyrosine 39 is Essential for Wild-Type-Like Covalent Aggregation of Native α -Synuclein.

To determine how each tyrosine contributes to covalent aggregation, seven variants, each containing two or three tyrosines, were reacted with cytochrome *c* and H₂O₂. The conditions used do not promote non-covalent aggregation of α -synuclein. Figure 3.3A shows the reaction between cytochrome *c* and H₂O₂ as a standard. Figure 3.3B shows the participation of each tyrosine in oxidative aggregation. When tyrosine 125, 133, or 136 is removed (Figure

3.3B, lanes 3-5), covalently aggregated species are populated in the same manner as for the wild-type protein (lane 1). When the least reactive tyrosine, tyrosine 39, is removed (Figure 3.3B, lane 2), even-numbered aggregates (dimer, tetramer, and perhaps hexamer and octamer) are favored over the trimer. In general, more uniform covalent aggregate populations are observed when α -synuclein has at least one tyrosine at each end. This observation is supported by the data in Figure 3.3C, where variants with tyrosine 39 and one other tyrosine are examined.

3.2.4 Changes in Covalent Aggregation Induced by a Denaturant.

If α -synuclein were totally disordered, one would expect that wild-type-like covalent aggregation could be achieved if any two tyrosines are present. However, as shown in Figure 3.3, tyrosine 39 is essential for wild-type-like covalent aggregation. To determine if protein conformation was the basis of this observation, wild-type α -synuclein or the variant with tyrosine 39 removed were reacted with cytochrome *c* and H_2O_2 in the presence and absence of the denaturant, guanidine hydrochloride (300 mM). A control experiment (not shown) illustrates that 300 mM guanidine hydrochloride does not affect radical formation as assessed by the bands formed in cytochrome *c* covalent aggregation with and without guanidine hydrochloride. Coomassie Blue staining was used because guanidine hydrochloride interferes with Alexa Fluor fluorescence. In the presence of guanidine hydrochloride (Figure 3.4B-C, lane 2), large covalent aggregates are more heavily favored for both wild-type and Y39F α -synuclein compared to the reaction in the absence of guanidine hydrochloride

(Figure 3.4B-C, lane 1). In agreement with NMR-based experiments, these data show that α -synuclein must have some structure that can be destroyed by a denaturant (5).

3.2.5 Fibril Formation and Oxidative Aggregation.

To determine if covalent aggregation affects the conformation required for non-covalent fibril formation, fibrils were grown from the wild-type protein. Coomassie Blue staining was used because the fibril growth conditions interfere with Alexa Fluor fluorescence. As a control, either cytochrome *c* or H_2O_2 were added either at the start or end of fibril growth. In each of these conditions, no covalent aggregates were detected in the supernatant or in the fibrils (data not shown). Figure 3.5B shows the effects of exposing the fibrillization reaction to cytochrome *c* and H_2O_2 at the beginning or at the end of fibril growth. When peroxidation is introduced after 24 h of fibril growth (lanes 3 and 4), the covalent aggregates are observed in both the supernatant and the fibrils, and a large fibril pellet is observed. When peroxidation is introduced early, almost no fibrils are formed (as indicated by a miniscule pellet) and there is nearly a complete absence of covalent aggregates (lane 2). Instead, nearly all of the covalent aggregates are found in the supernatant (lane 1). Similar results are obtained for the variant containing only the tyrosine 39 to phenylalanine mutation (although the yield of fibrils is lower).

3.4 Discussion

The present studies examine the role of α -synuclein conformation in its peroxidative aggregation. The conformations of this intrinsically disordered

protein have been characterized by NMR, and the shape shown in Figure 1B is just one of an ensemble of collapsed conformations adopted by α -synuclein (5). While the protein does not have a rigid secondary structure, these conformations have similar characteristics, namely that the charged termini collapse onto the hydrophobic core. In each conformation, the region surrounding tyrosine 39 abuts the core and C-terminus. This contact keeps tyrosine 39 partially protected from the solvent, which accounts for its low reactivity (Figure 3.2). NMR-detected amide-proton exchange experiments also show that tyrosine 39 is protected from the solvent, as indicated by its low exchange rate (6). In each conformation, the region surrounding tyrosine 125 contacts three other regions (residues 11-13, 30-75, and 78-99) (7). Tyrosine 125 is in a region of increased rigidity compared to the rest of the protein (5, 7, 8), although the C-terminus as a whole is comparatively mobile. This synergy of rigidity and flexibility accounts for the decreased reactivity of tyrosine 125 compared to tyrosines 133 and 136, and its increased reactivity compared to tyrosine 39 (Figure 3.2).

The collapsed conformation of α -synuclein explains why at least one tyrosine on each end of the protein is required to maintain a distribution of covalent aggregates similar to that observed for the wild-type protein (Figure 7A). When C-terminal tyrosines from two α -synuclein monomers react, the collapsed conformation sterically hinders the two remaining C-terminal tyrosines from reacting (Figure 3.6B and 3.6C). Without a tyrosine near the N-terminus, i.e. tyrosine 39, dimers are favored (Figure 3.6B), but once a sufficient population of dimers accumulates, they tend to form tetramers, hexamers, and higher-order

even-numbered aggregates (Figure 3.6C). The lower reactivities of tyrosines 39 and 125 (Figure 3.2) explain why variants with only these tyrosines (Figure 3.3C, lane 1) tend to form fewer higher-order covalent aggregates. When α -synuclein is denatured with guanidine hydrochloride, an N-terminal tyrosine is no longer needed for wild-type-like covalent aggregation (Figure 3.6D) because the three C-terminal tyrosines are more accessible.

α -Synuclein must undergo a folding event to form an aggregation nucleus (9) before forming fibrils (Figure 3.6E). Covalently cross-linking the protein's tyrosines prevents it from folding properly, so that, as shown in Figure 3.5, covalent aggregates are not incorporated into fibrils. In addition, when oxidation is introduced at the start of the fibrillization process, little to no fibril growth is observed because the concentration of monomer is too low to allow fibrillization in the time frame of the experiment. Once fibrils have assembled (Figure 3.6E), however, the termini are stacked (10) so that the tyrosines are solvent-exposed and accessible for oxidative cross-linking. While tyrosine 39 is essential for fibril formation (11), an N-terminal tyrosine is not required for covalent aggregation within fibrils. This observation is similar to that which is observed when the protein is denatured by guanidine hydrochloride. In summary, my data indicate that both covalent and non-covalent aggregation of α -synuclein depend on its conformation and suggest that covalent aggregation occurs in Lewy bodies after the formation of fibrils

3.5 Figures and Tables

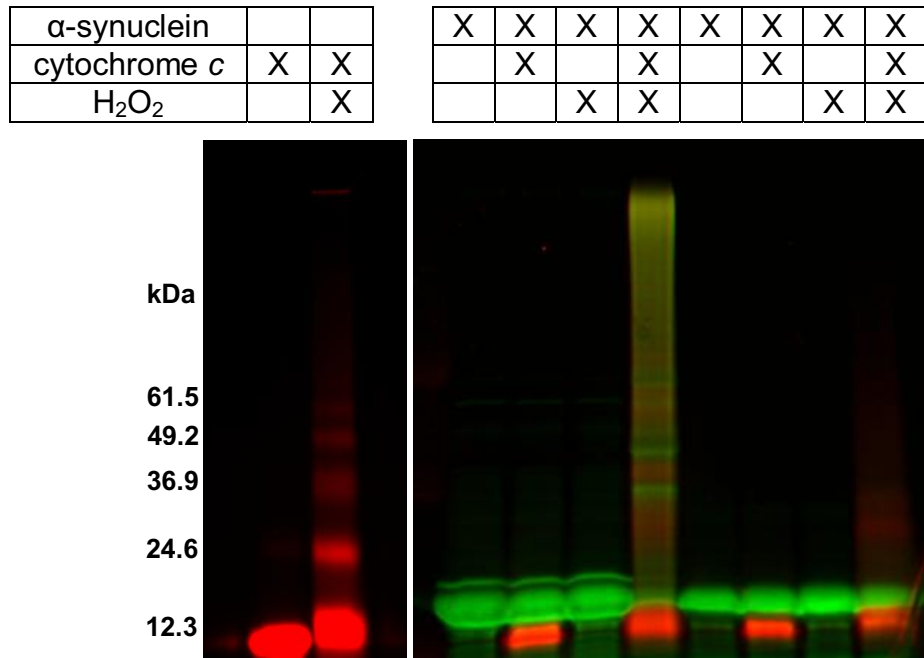


Figure 3.1 Alexa Fluor labeling detects peroxidative aggregation.

Panel A: Cytochrome c was incubated with and without H₂O₂. **Panel B:** α -Synuclein, either the wild-type protein with the Alexa Fluor label at position 3 (WT, lanes 1-4), or a no tyrosine variant with the Alexa Fluor label at position 3 (noY, lanes 5-8) were combined with various combinations of cytochrome c and H₂O₂ for 90 min., separated on a 10-20% gradient polyacrylamide gel, and visualized by fluorescence (green, α -synuclein; red, cytochrome c).

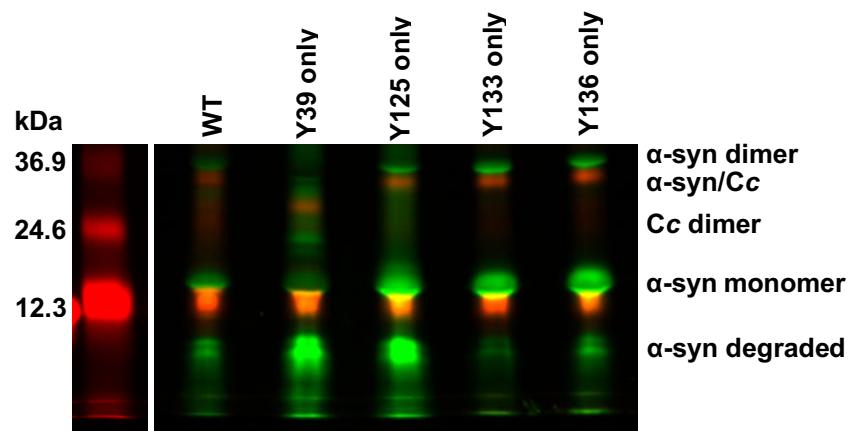


Figure 3.2 Every tyrosine in α -synuclein is reactive, but to varying extents.

Panel A: Cytochrome *c* was incubated with H_2O_2 . **Panel B:** The wild-type protein (WT) and single tyrosine-containing variants of α -synuclein were reacted with cytochrome *c* and H_2O_2 for 90 minutes, and treated as described in the caption to Figure 2.

Y39	X		X	X	X
Y125	X	X		X	X
Y133	X	X	X		X
Y136	X	X	X	X	

X	X	X
X		
	X	
		X

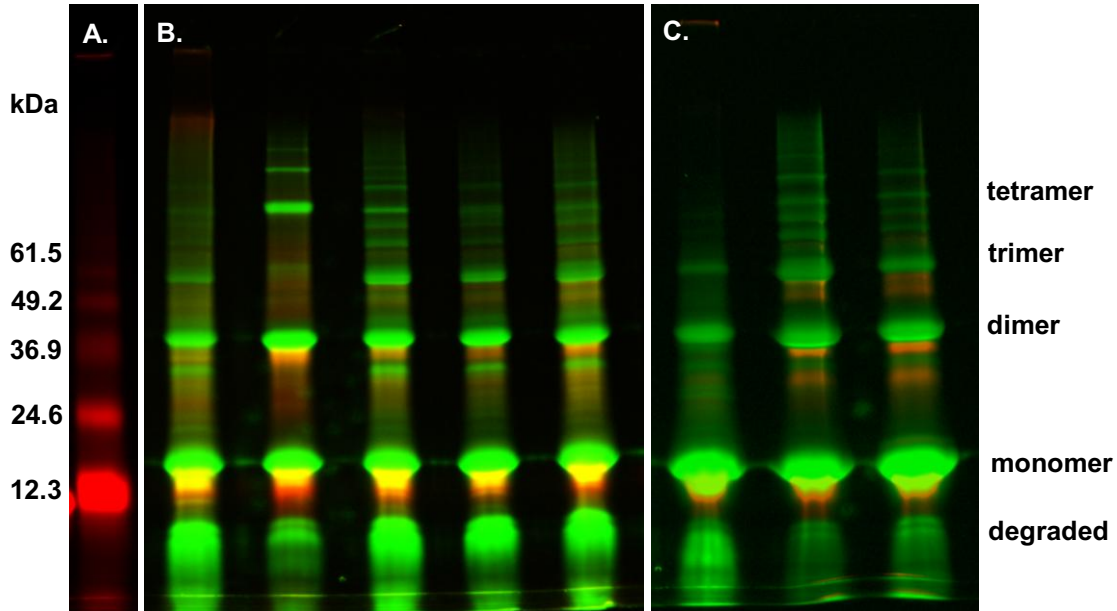


Figure 3.3 At least one tyrosine on each end is required for wild-type-like covalent aggregation of collapsed α -synuclein. **Panel A:** Cytochrome *c* was incubated with H_2O_2 . **Panel B:** The wild-type protein and variants containing three tyrosines or **Panel C:** two tyrosines were reacted with cytochrome *c* and H_2O_2 for 90 minutes, and treated as described in the caption to Figure 2. Legend at top indicates which tyrosines are present in each variant. α -Synuclein aggregate species are indicated on the right.

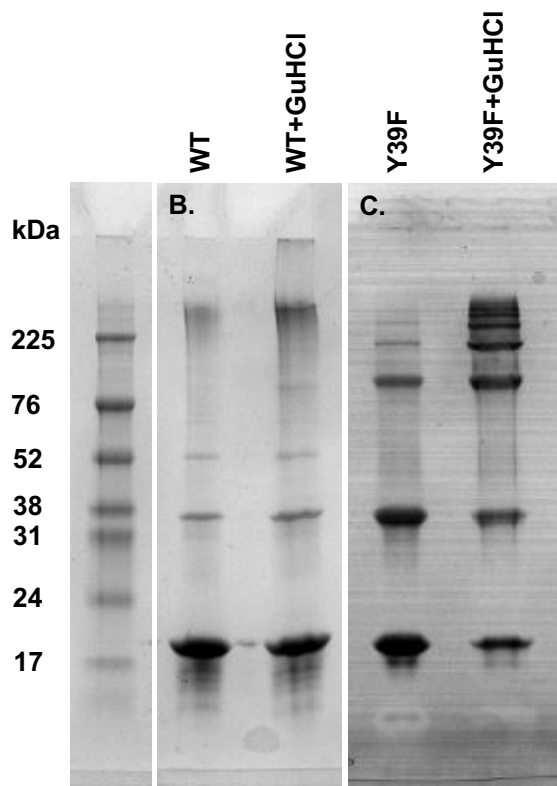


Figure 3.4 Tyrosine 39 is not required for full aggregation of denatured α -synuclein. **Panel A:** Molecular weight marker. **Panel B:** The wild-type protein (WT) and **Panel C:** the variant with tyrosine 39 removed (Y39F) were reacted with cytochrome *c* and H_2O_2 in the presence (lanes 2) or absence (lanes 1) of guanidine hydrochloride. Samples were separated on a 10-20% gradient polyacrylamide gel, and visualized by Coomassie Blue staining.

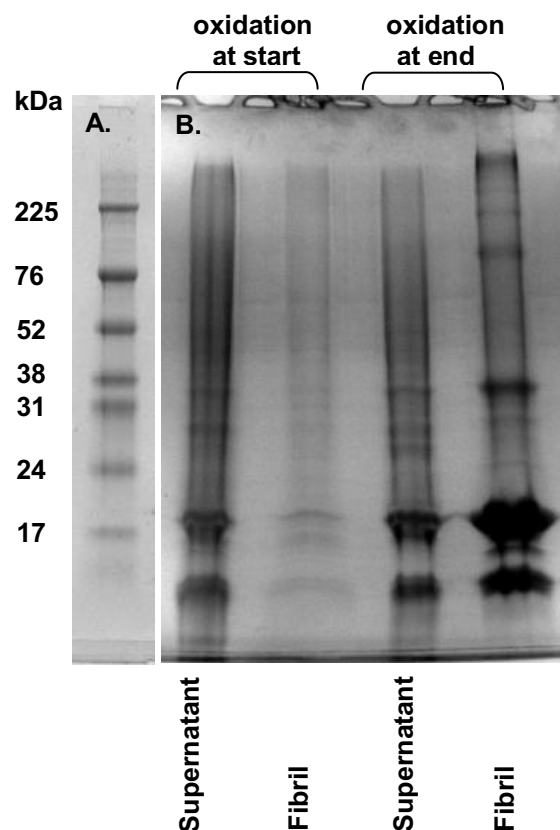


Figure 3.5 Oxidative aggregation interferes with fibril formation. **Panel A:** Molecular weight marker. **Panel B:** The wild-type protein was reacted with cytochrome c and H_2O_2 before (lanes 1 and 2) or after (lanes 3 and 4) fibril formation. Fibrils were isolated by centrifugation. Fibrils (lanes 2 and 4) and the supernatant (lanes 1 and 3) were boiled with SDS, separated on 10-20% gradient polyacrylamide gels, and visualized with Coomassie Blue.

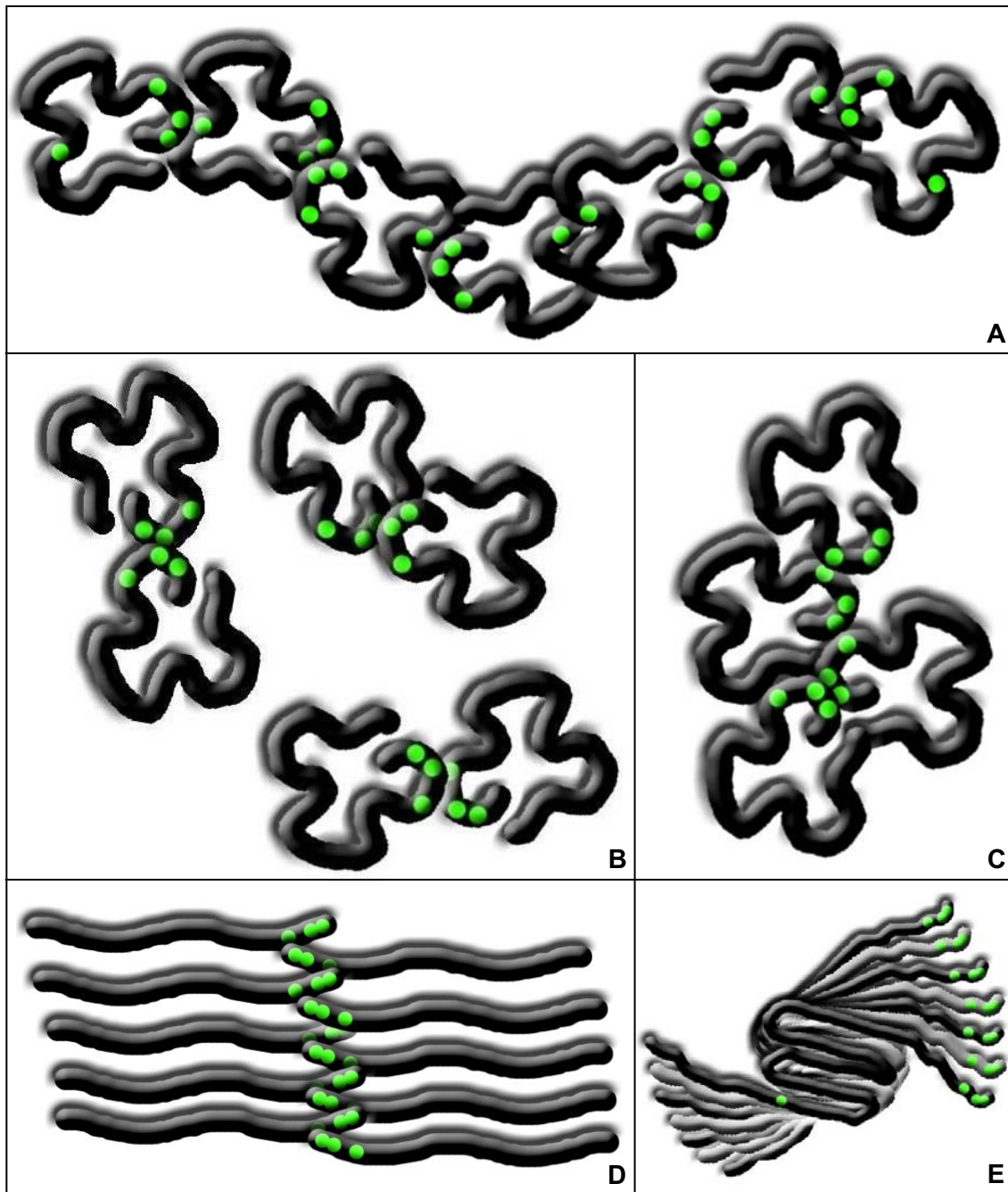


Figure 3.6 α -Synuclein conformation and covalent aggregation. **Panel A:** When α -synuclein adopts a collapsed conformation, various covalently aggregated species are more equally populated when at least one tyrosine is present on each end of the protein. **Panels B and C:** Even-numbered aggregates are favored when tyrosine 39 is removed. **Panel D:** When α -synuclein is completely disordered, the largest aggregate species are favored, even if tyrosine 39 is removed. **Panel E:** Covalent α -synuclein aggregates are unable to fold into the beta-sheet aggregation nucleus, but once the folded monomers have assembled into protofibrils, the termini are stacked, allowing covalent aggregation of any of the tyrosines.

3.6 References

1. Olteanu, A. and Pielak, G. J. (2004) Peroxidative aggregation of α -synuclein requires tyrosines, *Protein Sci.* **13**, 2852-2856.
2. Shigenaga, M. K., Hagen, T. M. and Ames, B. N. (1994) Oxidative damage and mitochondrial decay in aging, *Proc. Natl. Acad. Sci. U. S. A.* **91**, 10771-10778.
3. Lashuel, H. A., Hartley, D., Petre, B. M., Walz, T. and Lansbury, P. T., Jr. (2002) Amyloid pores from pathogenic mutations, *Nature* **418**, 291.
4. Lardinois, O. M., Tomer, K. B., Mason, R. P. and Deterding, L. J. (2008) Identification of protein radicals formed in the human neuroglobin—H₂O₂ reaction using immuno-spin trapping and mass spectrometry, *Biochemistry* **47**, 10440-10448.
5. Bertoncini, C. W., Jung, Y. S., Fernandez, C. O., Hoyer, W., Greisinger, C., Jovin, T. M. and Zweckstetter, M. (2005) Release of long range tertiary interactions potentiates aggregation of natively unstructured alpha-synuclein, *Proc. Natl. Acad. Sci. U. S. A.* **102**, 1430-1435.
6. Croke, R. L., Sallum, C. O., Watson, E., Watt, E. D. and Alexandrescu, A. T. (2008) Hydrogen exchange of monomeric α -synuclein shows unfolded structure persists at physiological temperature and is independent of molecular crowding in *Escherichia coli*, *Protein Sci.* **17**, 1434-1445.
7. Dedmon, M. M., Lindorff-Larsen, K., Christodoulou, J., Vendruscolo, M. and Dobson, C. M. (2004) Mapping long-range interactions in alpha-synuclein using spin-label NMR and ensemble molecular dynamics simulations, *J. Am. Chem. Soc.* **127**, 476-477.
8. Bussell Jr., R. and Eliezer, D. (2001) Residual structure and dynamics in Parkinson's disease associated mutants of alpha synuclein, *J. Biol. Chem.* **276**, 45996-46003.
9. Shahi, P., Sharma, R., Sanger, S., Kumar, I., Jolly, R.S. (2007) Formation of amyloid fibrils via longitudinal growth of oligomers, *Biochemistry* **46**, 7365-7373.

10. Vilar, M., Chou, H.-T., Luhrs, T., Maji, S. K., Riek-Loher, D., Verel, R., Manning, G., Stahlberg, H. and Riek, R. (2008) The fold of α -synuclein fibrils, *Proc. Natl. Acad. Sci. U. S. A.* **105**, 8637-8642.
11. Ulrikh, N. P., Barry, C. H. and Fink, A. L. (2008) Impact of Tyr to Ala mutations on α -synuclein fibrillation and structural properties, *Biochim. Biophys. Acta* **1782**, 581-585.

Chapter 4 Progress Towards Neuronal Microinjection of Aggregated α -Synuclein

4.1 Introduction

As described in Chapter 1, the aggregation of α -synuclein is a critical but poorly understood process in Parkinson's disease. Currently it is not known which aggregated form is most toxic *in vivo*, but *in vitro* evidence points towards the protofibril, particularly the annular or ring-shaped form (1). Some studies have shown that α -synuclein aggregates are toxic to cells, but these studies are insufficient for several reasons (2-4). In all experiments, cells were made to express α -synuclein by transfection, in which the level of protein expression is not controlled. This process does not lend itself to quantitative analysis of aggregate toxicity because a controlled amount of aggregate cannot be introduced to the cells. Also, these experiments exposed the cells to a mixture of aggregate species, not specific aggregates. Furthermore, these experiments did not address the question of whether oxidative stress is a cause of aggregation, a product of aggregation, or both.

Neuronal microinjection is an ideal technique to combat these problems (5). Briefly, specific neurons are harvested from neonatal mice and cultured on adherent plates. Protein samples are injected into individual cells and cell

viability is measured as a function of time. The components of the culture media and/or injection sample can be modified as required to mimic cellular processes such as oxidative stress or dopamine processing. Overall, neuronal microinjection allows measurements of the concentration-dependant toxicity of individual aggregate species under a variety of cellular conditions.

When beginning a new protocol, especially one that involves animals, it is imperative that all controls and procedures be established before data collection begins. To that end, this chapter details the progress toward sample preparation and oxidative stress induction and detection.

4.2 Sample Preparation

4.2.1 Cell Adherence

Neuronal microinjection is usually conducted with cells adhered to a 35-mm plastic culture dish with collagen. Glass-bottomed culture dishes are required because quantitative fluorescence analysis is needed to measure oxidative stress in the cells. Three types of plates were tested: freshly collagen-coated, collagen-coated by the manufacture (MatTek, Ashland, Massachusetts), and freshly lysine-coated. Superior cervical ganglion neurons only adhere to the freshly collagen-coated plates. Also, if freshly-coated plates are stored for more than a few hours, even at 4°C, neurons no longer adhere to them.

Interestingly, even though cells adhere to freshly collagen-coated plates, the collagen itself does not adhere well to the glass of the plate. Typically, the collagen is applied to the plate via a disposable dropper pipette, which does not allow consistent deposition. Also, the glass-bottomed plates have a smaller area

than the plastic plates, so one drop of collagen makes a thicker layer on glass that may not dry evenly, leading to poor adherence. In addition, it is critical that the collagen layers are uniform so that the cells adhere in the horizontal plane for imaging. To address these issues, the collagen was applied in two layers using volumes of either of either 50 or 25 μL . The plates were allowed to air-dry for at least 2 hours between applications. The 50- μL application is too thick to adhere properly to the glass, but the 25- μL application adheres well. Although the two-layer application increases adherence of the collagen layer, it also causes uneven collagen that disrupts cell adhesion. In the end, one 25- μL collagen layer, carefully spread with a glass stir rod on a glass-bottom culture dish, provides the best combination of collagen adhesion, collagen uniformity, and cell adhesion.

4.2.2 Growth Medium

Initially, cells were grown in AM50 medium [minimum essential medium (MEM) without phenol red (Gibco, Invitrogen) supplemented with 10% fetal bovine serum, 2- μM uridine (Sigma, St. Louis, Missouri), 2- μM fluorodeoxyuridine (Sigma), 100 $\mu\text{g}/\text{mL}$ penicillin (Gibco), 100 $\mu\text{g}/\text{mL}$ streptomycin (Gibco), and 50 ng/mL murine nerve growth factor 7S (Promega, Madison, Wisconsin)]. This medium contains no antioxidants, and therefore the cells are susceptible to oxidative stress, especially when being transported between labs. To correct this, the AM50 growth medium was supplemented with 50- μM α -tocopherol (vitamin E), which has been shown to protect neurons against oxidative stress (6).

Oxidative stress induction and detection are discussed in more detail later, but briefly, the cells are grown in the test medium for 4-7 days, and then washed thoroughly with MEM. Oxidative stress is induced in the positive control plates, which are washed again with MEM before oxidative stress detection. As seen in Figure 4.1, the addition of vitamin E gives mixed results on measuring oxidative stress. In AM50 medium, the variance between samples of the same type is small (0-0.8%), the variance within one sample is small (0-2.5%), and the values of the negative control (0%) and positive control (6.0-6.8%) are statistically different. However, the difference between the positive and negative controls is small. Conversely, in medium supplemented with vitamin E, the variance between samples of the same type is large (9%), the variance within one sample is large (1.8-13.3%), and the values of the negative control (1.8%) and positive control (3.9-12.9%) are statistically the same. This large variance may be due to vitamin E's high hydrophobicity; it may not dissolve fully in the AM50 medium, causing cells to receive varying amounts of the antioxidant. However, several hydrophilic antioxidants, including ascorbic acid (vitamin C), phenol red, and trolox (a water-soluble form of vitamin E), may prove effective in preventing oxidative stress during the growth of the neurons and thereby allow a greater response to induced oxidative stress in the positive controls.

4.2.3 Alexa Fluor Labeling of α -Synuclein

As discussed in Chapter 2, Alexa Fluor labeling of α -synuclein is an efficient method for fluorescently tagging the protein. In this experimental design, there are several parameters to consider when choosing the specific Alexa Fluor

dye. The three fluorescent microscopes used for microinjection, cell counting, and oxidative stress measurement/cell imaging all have the standard blue, green, and red filter sets, albeit they have a slightly different range on each microscope. As described in more detail below, the blue channel is used for Hoechst dye (a DNA marker) and the green for 5-(and-6)-carboxy-2',7'-dichlorodihydro-fluorescein diacetate (an oxidative stress fluorogenic marker), leaving the red channel for Alexa Fluor. Of the Alexa Fluor maleimides, two (Alexa Fluor 555 and Alexa Fluor 568) are compatible with the red channel. Both dyes label α -synuclein to an acceptable degree (~90% for Alexa Fluor 555 and ~75% for Alexa Fluor 568). Alexa Fluor 568 was ultimately chosen for its higher fluorescence intensity on the cell counting microscope because cell counting is done by eye.

4.3 Oxidative Stress Induction and Detection

4.3.1 Inducing Oxidative Stress for Positive Control

Tert-butyl-hydroperoxide (TBHP) was used as a positive control for oxidative stress-induction. I noticed a decrease in the number of oxidative stress-positive cells in the positive control plates with time. To determine if the age or concentration of TBHP was a factor in the decrease, I compared the original sample (approximately 6 months old) with a newly prepared 100 mM-stock solution, both diluted to a working solution at the original concentration (100 μ M) and a higher concentration (200 μ M). As seen in Figure 4.2, both the age of the stock solution and the concentration of the working solution play a role in the amount of oxidative stress induced. The older TBHP sample induced

oxidative stress in only 0.4-1.1% of the cells, compared to 1.6-3.1% using the freshly prepared sample and 9.0-9.8% at the higher concentration. This same sample was used 25 days later (the AM50 data in Figure 4.2) and only induced oxidative stress in 6.0-6.8% of the cells. These observations indicate that TBHP has a short shelf life. A fresh stock solution must be prepared for every experiment the stock should not be frozen (7).

4.3.2 Fluorogenic Oxidative Stress Marker Selection

Dozens of fluorogenic markers that detect various forms of oxidative stress are commercially available. For the purposes of these experiments, the marker must possess the following criteria: 1) detect oxidative stress in living cells, 2) emit fluorescence detectable with the filter sets on the available microscopes, 3) have a proportional response to the amount of oxidative stress and 4) ,ideally, detect a wide range of reactive oxygen species. Based on the first parameter, six markers were chosen for study.

As seen in Table 4.1, diphenyl-1-pyrenylphosphine fails criterion 2 because no fluorescence was detected in the negative control cells, the positive control cells, or the background. MitoTracker, reduced MitoTracker, RedoxSensor Red, and Amplex Red all fail criterion 3 because the positive and negative controls have approximately the same number of oxidative stress-positive cells. Ultimately, Image-iT [5- (and 6-) carboxy-2',7'-dichlorodihydro-fluorescein diacetate] was chosen because it possesses all of the necessary criteria.

4.3.3 Staining Procedure

To measure oxidative stress in the cells, the cells must be transported from the growth lab to the imaging lab, an approximately 15-min walk across campus. Initially, the cells were transported in a commercially prepared hibernation medium (Hibernate E, Brain Bits, Springfield, Illinois) to preserve them in the ambient CO₂ conditions. The cells were stained with Image-iT and Hoechst dye at the imaging lab. They were then washed with MEM before imaging with an inverted fluorescence microscope (DMIRB, Leica, Wetzlar, Germany) fitted with an OrcaER camera (Hamamatsu, Sewickley, Pennsylvania) and SimplePCI software (Hamamatsu). Although a quantitative analysis could not be performed due to a lack of background correction, a qualitative analysis confirmed the prior assessment that TBHP induces Image-iT detectable oxidative stress (Figure 4.3).

Staining the cells at the imaging facility is difficult due to lack of proper equipment and space. Also, the phenol red present in the hibernation medium may counteract the induced oxidative stress. For the second test, the cells were stained in the growth lab with Image-iT diluted in MEM, transported to the imaging lab in the same medium, then washed and imaged as described above, with the addition of the proper background correction controls. Surprisingly, the negative controls showed a high level of stress and the positive controls a low level (Figure 4.4). It is unclear whether exposure to low CO₂ levels during transport or the staining procedure itself is responsible for this effect.

For the final experiment, half of the cells were stained in the growth lab with Image-iT diluted in hibernation medium lacking phenol red and half were

transported to the imaging lab in hibernation medium lacking phenol red and then stained. Then all cells were washed and imaged as described above. As shown in Figure 4.5, transportation in hibernation medium lacking phenol red followed by staining with Image-iT at the imaging facility results in a low response in the negative control and a high response in the positive control. These staining procedures were used for all subsequent experiments, including the data shown in Figures 4.1 and 4.2.

4.4 Conclusions

Now that the parameters have been established for growing neurons, labeling α -synuclein, and inducing and measuring oxidative stress within cells, the final parameter to set is the production and isolation of α -synuclein aggregate species. As shown in Chapters 2 and 3, I have already established a procedure for growing and purifying the fibril form. Fortunately, many procedures to produce both spherical and annular protofibrils have been described in the literature (8-11). I am confident that once a procedure for generating aggregates has been established, neuronal microinjection will prove to be a powerful tool to determine the toxicity of α -synuclein aggregates and what role oxidative stress plays in that process.

4.5 Figures and Tables

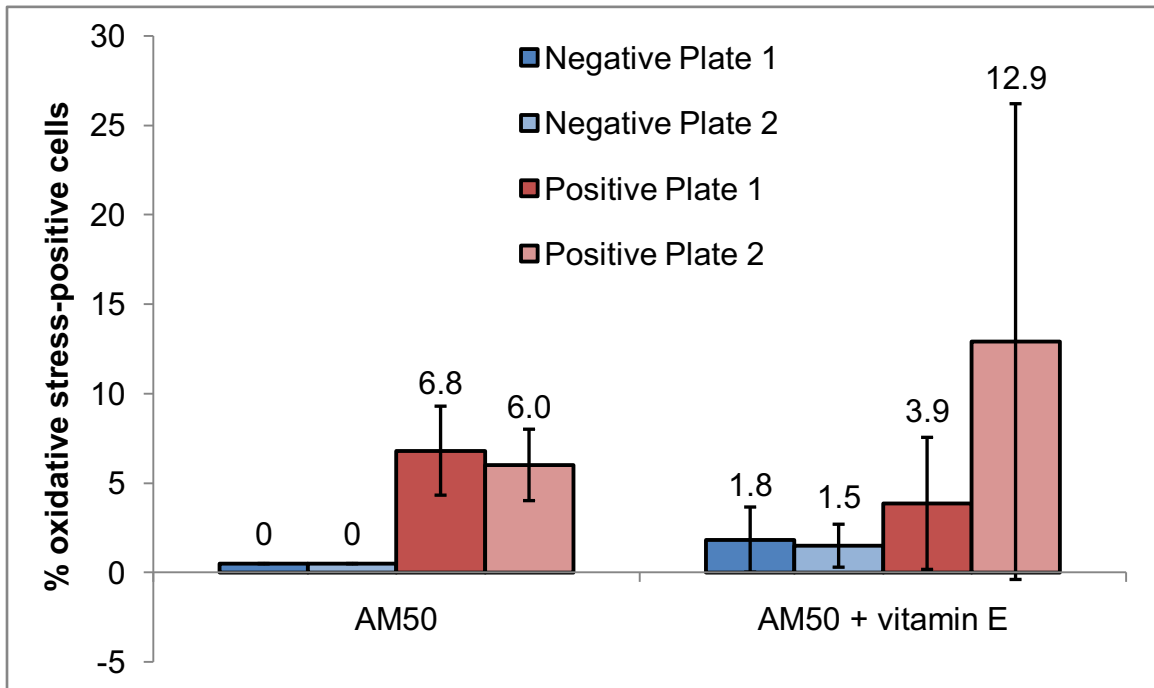


Figure 4.1 Vitamin E-supplemented growth media modulates neuronal response to oxidative stress. Superiour cervical ganglion cells were grown in AM50 media with or without 50- μ M vitamin E for 4 days. The cells were washed with MEM and the positive control cells were stressed with 200- μ M TBHP in MEM for 180 min. Cells were washed with MEM, transported in hibernation medium without phenol red, and stained with Image-iT. While the vitamin E facilitates a difference between the negative and positive controls, it also causes a high variance between samples. Error bars represent the standard deviation of nine images collected per sample. An average of 230 cells were counted per image. (Blue bars, negative control; Red bars, positive control; light and dark are different plates of the same type)

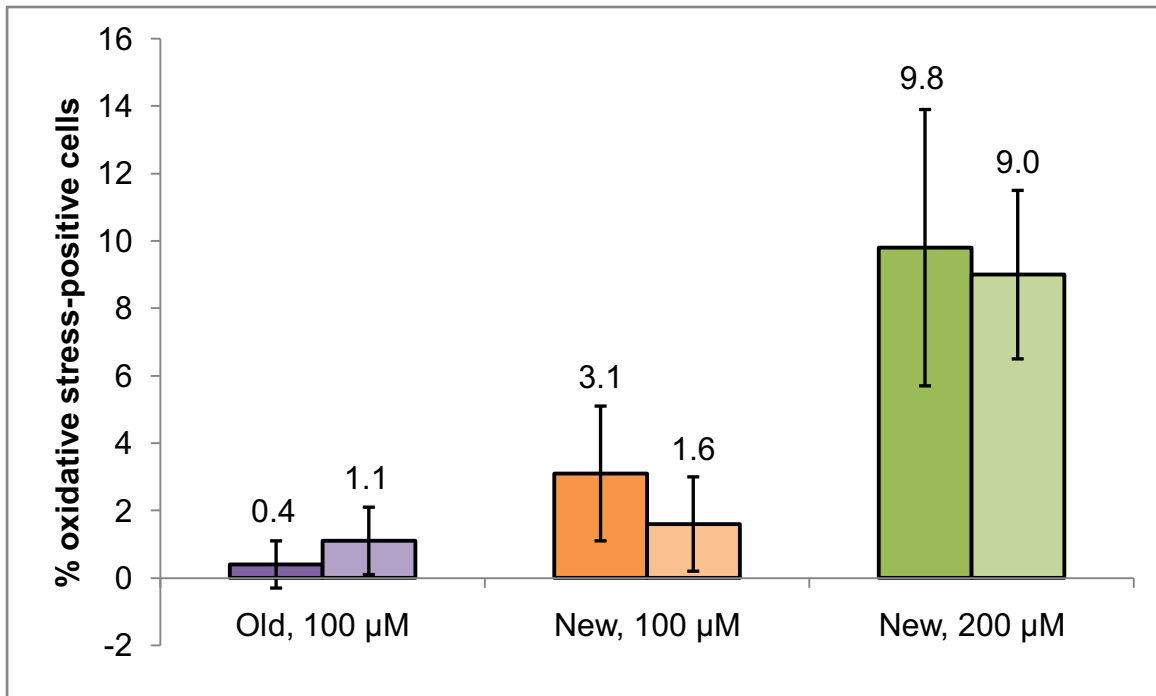


Figure 4.2 Age of stock solution and concentration of working solution affect the ability of TBHP to induce oxidative stress. Cells were stressed with either old (6 months) TBHP stock at 100 μ M working concentration, fresh TBHP stock at 100 μ M working concentration, or fresh TBHP stock at 200 μ M working concentration. The cells were washed with MEM, transported in hibernation medium without phenol red, and stained with Image-iT. Fresh TBHP and increased TBHP concentration both improve the effectiveness of TBHP at inducing oxidative stress. Error bars represent the standard deviation of three images collected per sample. An average of 70 cells were counted per image. Light and dark bars are different plates of the same type.

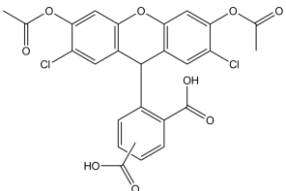
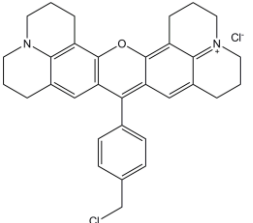
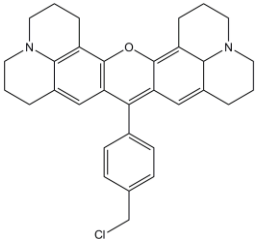
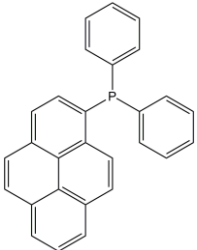
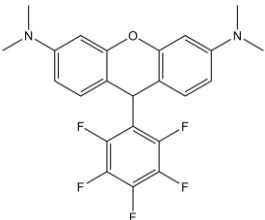
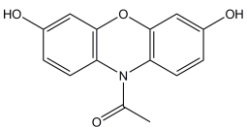
Trade Name	Structure	Detects	Negative Control	Positive Control
Image-iT		ROS	Cells: low Background: moderate	Cells: high Background: moderate
Mito Tracker		ROS	Cells: moderate Background: moderate	Cells: moderate Background: moderate
Reduced Mito Tracker		ROS	Cells: moderate Background: high	Cells: moderate Background: high
diphenyl-1-pyrenyl-phosphine		H ₂ O ₂	Cells: none Background: none	Cells: none Background: none
Redox Sensor Red		ROS	Cells: moderate Background: moderate	Cells: moderate Background: moderate
Amplex Red		H ₂ O ₂	Cells: none Background: high	Cells: none Background: high

Table 4.1 Fluorogenic markers to detect oxidative stress.

ROS, reactive oxygen species; Cells, amount of fluorescence detected in cells; Background, amount of fluorescence detected outside of cells

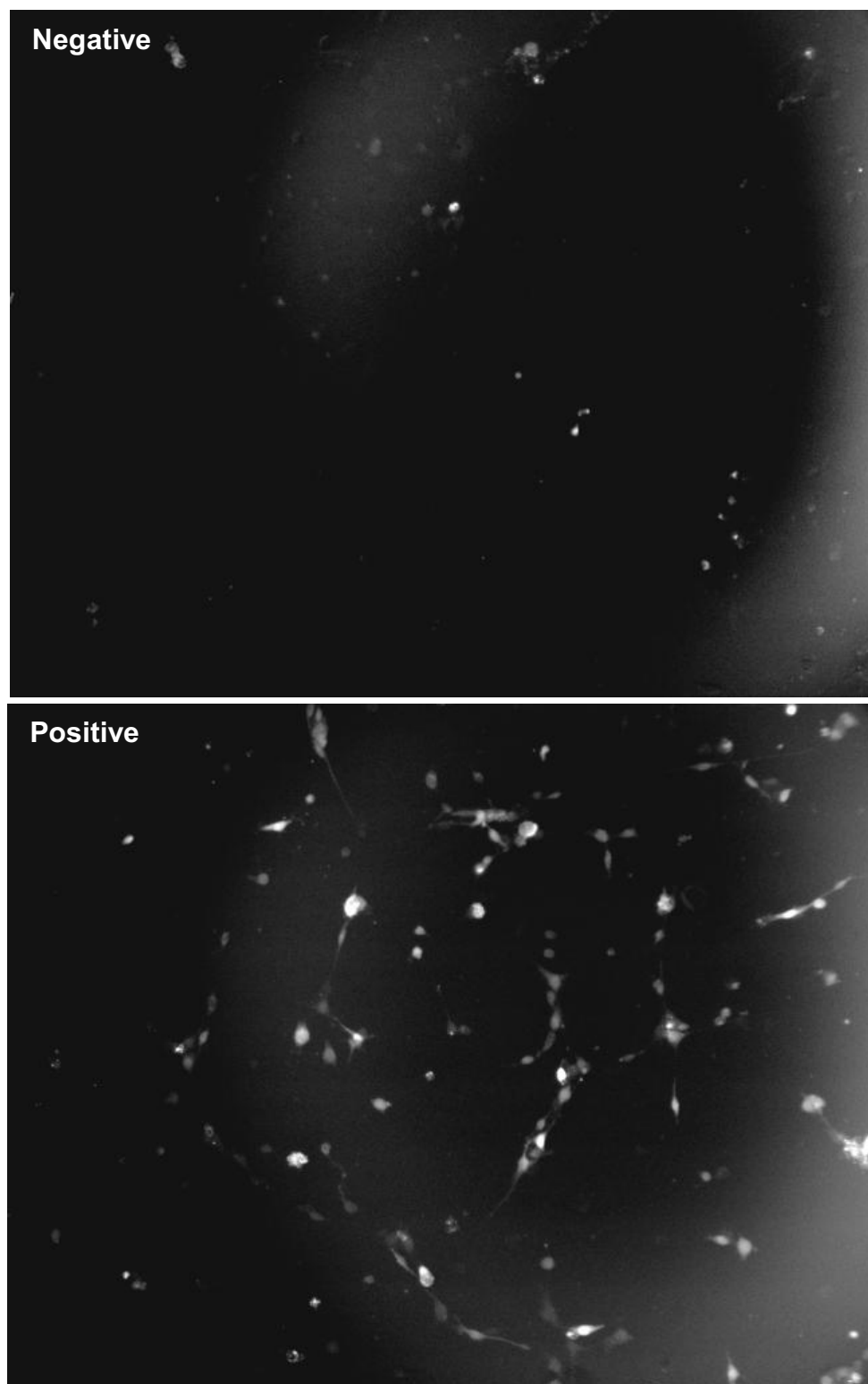


Figure 4.3 TBHP causes increased oxidative stress in cells.

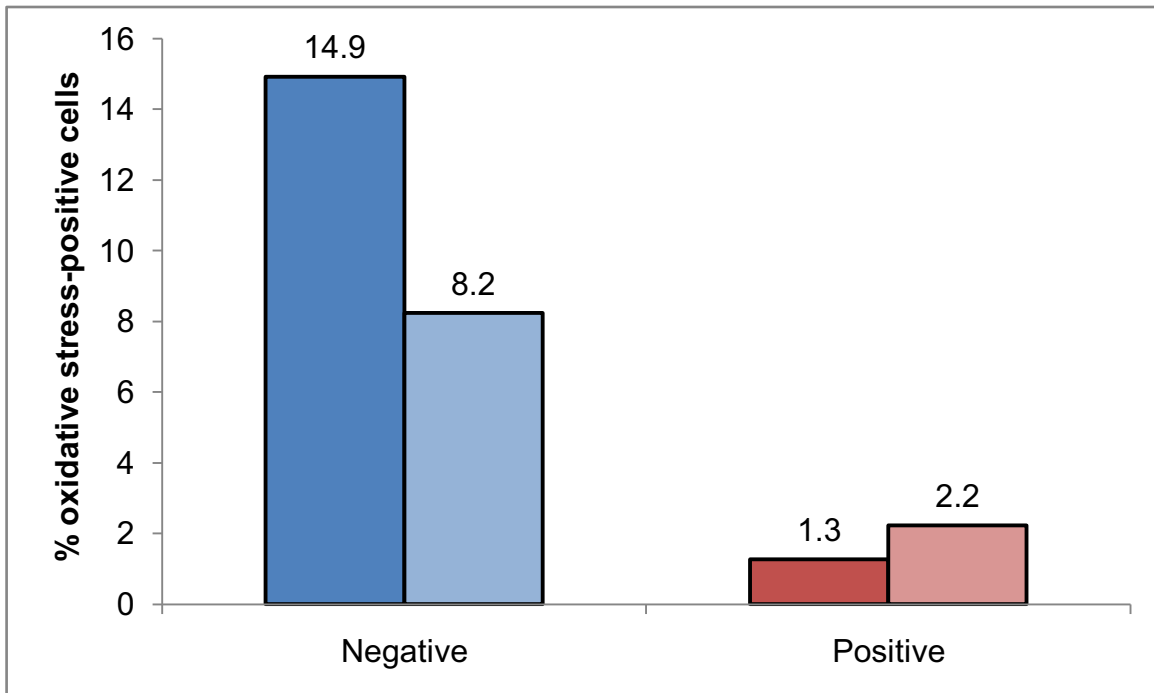


Figure 4.4 Transporting cells in staining solution reverses the expected results. Positive control cells were stressed with 200- μ M TBHP in MEM for 180 minutes. All cells were washed with MEM, stained with Image-iT diluted in MEM, and transported to imaging lab. The negative controls show a high level of stress and the positive controls a low level, which contradicts what is expected. An average of 200 cells were counted per image. (Blue bars, negative control; Red bars, positive control; light and dark are different plates of the same type)

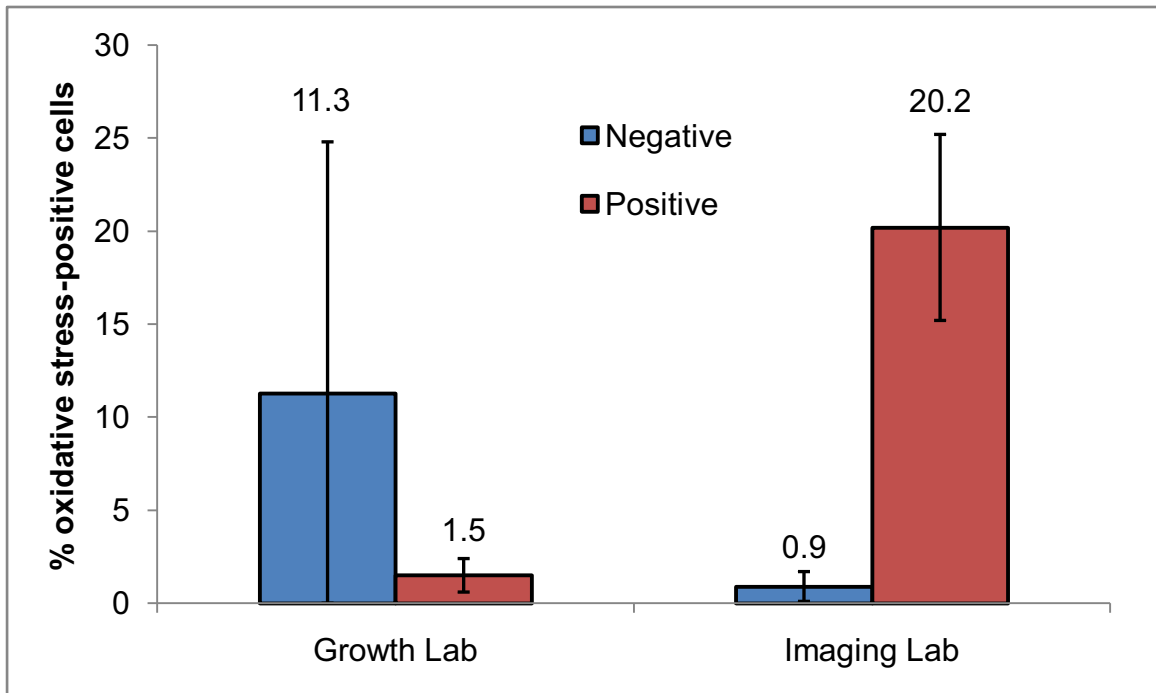


Figure 4.5 Transport in hibernation media and staining immediately prior to imaging are crucial for proper oxidative stress detection. Cells were either stained in the growth lab with Image-iT diluted in hibernation medium lacking phenol red (Growth Lab) or transported to the imaging lab in hibernation medium lacking phenol red and then stained (Imaging Lab). Staining after transport is essential for accurate oxidative stress detection. Error bars represent the standard deviation of three images collected per sample. An average of 154 cells were counted per image. (Blue bars, negative control; Red bars, positive control; light and dark are different plates of the same type)

4.6 References

1. Lashuel, H. A., Petre, B. M., Wall, J., Simon, M., Nowak, R. J., Walz, T. and Lansbury, P. T. (2002) Alpha-synuclein, especially the Parkinson's disease associated mutants, forms pore-like annular and tubular protofibrils, *J. Molec. Biol.* **322**, 1089-1102.
2. Mazzulli, J. R., Mishizen, A. J., Giasson, B. I., Lynch, D. R., Thomas, S. A., Nakashima, A., Nagatsu, T., Ota, A. and Ischiropoulos, H. (2006) Cytosolic catechols inhibit α -synuclein aggregation and facilitate the formation of intracellular soluble oligomeric intermediates, *J. Neurosci.* **26**, 10068-10078.
3. Opazo, F., Krenz, A., Heermann, S., Schulz, J. B. and Falkenburger, B. H. (2008) Accumulation and clearance of α -synuclein aggregates demonstrated by time-lapse imaging, *J. Neurochem.* **106**, 529-540.
4. Roberti, M. J., Bertoncini, C. W., Klement, R., Jares-Erijman, E. A. and Jovin, T. M. (2007) Fluorescence imaging of amyloid formation in living cells by a functional, tetracycline-tagged α -synuclein, *Nature* **6**, 845-851.
5. Wright, K. M., Linhoff, M. W., Potts, P. R. and Deshmukh, M. (2004) Decreased apoptosome activity with neuronal differentiation sets the threshold for strict IAP regulation of apoptosis, *J. Cell Biol.* **167**, 303-313.
6. Numakawa, Y., Numakawa, T., Matsumoto, T., Yagasaki, Y., Kumamaru, E., Kunugi, H., Taguchi, T. and Niki, E. (2006) Vitamin e protected cultured cortical neurons from oxidative stress-induced cell death through the activation of mitogen-activated protein kinase and phosphatidylinositol 3-kinase, *J. Neurochem.* **97**, 1191-1202.
7. <http://probes.invitrogen.com/media/pis/mp36007.pdf>
8. Ding, T. T., Lee, S. J., Rochet, J. C. and Lansbury, P. T. (2002) Annular alpha-synuclein protofibrils are produced when spherical protofibrils are incubated in solution or bound to brain-derived membranes, *Biochemistry* **41**, 10209-10217.
9. Kaye, R., Head, E., Thompson, J. L., McIntire, T. M., Milton, S. C., Cotman, C. W. and Glabe, C. G. (2003) Common structure of soluble

amyloid oligomers implies common mechanism of pathogenesis, *Science* **300**, 486-489.

10. Lowe, R., Pountney, D. L., Jensen, P. H., Gai, W. P. and Voelker, N. H. (2004) Calcium (II) selectively induces alpha synuclein oligomers via interaction with the C-terminal domain, *Protein Sci.* **13**, 3245-3252.
11. Kaye, R., Pensalfini, A., Margol, L., Sokolov, Y., Sarsoza, F., Head, E., Hall, J. and Glabe, C. (2009) Annular protofibrils are a structurally and functionally distinct type of amyloid oligomer, *J. Biol. Chem.* **284**, 4230-4237.